



Image by Peter Rubin - ©2016 ASU

Jackie Arroyo Donjuan, Nickolas Loftus, Michael Gunnarson, Christian Lum

UC Davis

EAE 143A Winter 2022

Professor Stephen K Robinson

<b>Section 1: Introduction</b>	<b>3</b>
1.1 Background	3
1.1.1 16 Psyche	3
1.1.2 Vehicle Overview	4
1.2 Mission Objectives	5
1.3 Customer & Stakeholder Requirements	6
1.4 Concept of Operations	7
1.4.1 Timeline	7
1.4.2 Timeline Breakdown	7
1.5 Product Breakdown Structure	8
1.5.0 Flowchart	8
1.5.1 Bus	8
1.5.1.0 Broad Description of subsystems	8
1.5.1.1 SSL-1300 Bus	9
1.5.1.2 Propulsion	9
1.5.1.2.1 SPT-140 Thrusters	10
1.5.1.2.2 Xenon gas in pressure vessels	10
Cold gas thrusters	10
Nitrogen gas in pressure vessels	11
1.5.1.3 Power	11
Dual gimbaled 5 panel solar arrays.	11
Power Control unit (PCU)	11
Power Processing units (PPU)	11
Batteries	11
1.5.1.4 Communication	12
1.5.1.5 Thermal	12
1.5.1.6 Guidance, Navigation and Control (GN&C)	12
1.5.1.7 Psyche Compute Element	13
1.5.2. Payload	14
1.5.2.0 Broad Description of Science Payload	14
1.5.2.1 Multispectral Imagers	14
1.5.2.2 Neutron & Gamma Ray Spectrometers	15
1.5.2.3 Magnetometer	15
1.5.2.4 Deep Space Optical Communications	15
<b>Section 2: Background/Heritage</b>	<b>15</b>
2.1. Previous similar spacecraft designs	15
2.2. What's new about your spacecraft compared to previous	16
<b>Section 3: Design to Meet Requirements</b>	<b>17</b>

3.1. Psyche subsystem requirements	17
3.2. Part Modification and Analysis	18
3.2.0 Mission modification motivation	18
3.2.1 New Power Requirements for ROSA	20
3.2.2 Risks and uncertainties associated with changes	21
3.3. Trade study to identify ideal design candidates	21
3.3.1 Xenon COPV - MT Aerospace	21
3.3.2 Trade study of ROSA - Deployable Space Systems (Redwire Inc.)	24
<b>Section 4: Analyses</b>	<b>25</b>
4.1 Power Budget and Thrust Analysis	25
4.1.2. Assumptions, principles, methods used (with refs)	26
4.1.2.1 Assumptions	26
4.1.2.2 Principles	27
4.1.3. Math, models, code	28
4.1.3.1 Current Power Profile	28
4.1.3.2 New Power Profile	29
4.2 Mass Budget Analysis	30
4.3 Delta V / Orbital Destination	32
4.3.1 Increase Delta V of Psyche to allow Mission Extension	32
4.3.2. Assumptions, principles, and methods used	33
4.3.3. Math, models, code	33
4.3.4. Results: plots, discussion, confidence, weaknesses	36
4.3.5. Discussion of how the results are important	40
<b>Section 5: Test Plan to Check Analyses</b>	<b>41</b>
5.1. Tests that have been accomplished and create influence	41
5.2. Tests that will be executed based on Requirement	41
5.3. Shortcomings of ground-based testing	42
<b>Section 6: Conclusion/Discussion</b>	<b>43</b>
<b>References</b>	<b>44</b>
<b>Appendix A: COPV Manufacturer Information</b>	<b>46</b>
<b>Appendix B: Solar Cell Data</b>	<b>48</b>
<b>Appendix C: COPV Replacement and VCalculations</b>	<b>50</b>
<b>Appendix D: Orbital Mechanics Calculations</b>	<b>51</b>

# Section 1: Introduction

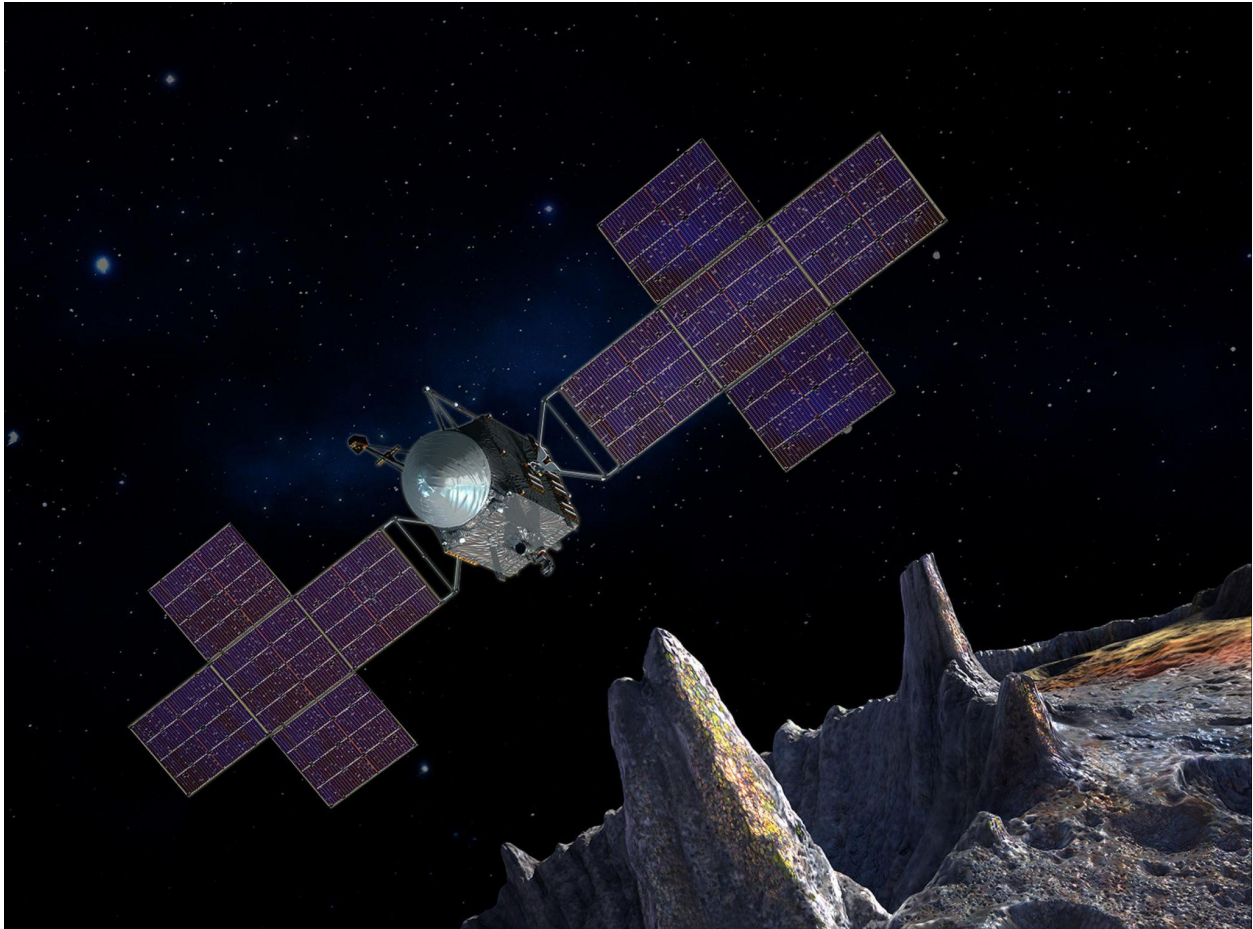


Figure 1: Artist Peter Rubin's Rendition of Psyche and (16) Psyche

## 1.1 Background

### 1.1.1 16 Psyche

(16) Psyche is a main belt asteroid first discovered in 1852 by Italian astronomer Annibale de Gasparis [1]. “16” prefix signifies that the asteroid was the sixteenth minor planet in order of discovery. No high resolution images of the asteroid are currently open source, but analysis of data acquired about it suggests that its shape is a triaxial ellipsoid (think squashed sphere with an elliptical shaped equator) [2]. Density and radar albedo measurements suggest that it is likely an M-type (metal) asteroid. (16) Psyche has an approximate diameter of 226 km, rotates on its axis in 4.196 hours, and orbits

the sun in 1 (16) Psyche years (5 earth years) at a distance of 2.5 to 3.3 astronomical units (AU). Its mass is estimated to be at least  $1.5 \times 10^{19} \text{ kg}$ [3].

It is theorized that (16) Psyche could be the exposed differentiated core of a now destroyed planet. During the solar-system's early development it is believed that many planetesimals were forming and colliding with each other. Some of these collisions may have destroyed one or both of the colliders, while others would have caused the two to fuse. As the planetesimals grew the radioactive material within them would cause their internals to melt. Their gravity would then cause them to differentiate, the heavier elements sinking to the core and lighter materials rising to the surface. The planetesimal that could have been the parent to (16) Psyche may have reached this point in its development only to have its outer layers stripped away by large impacts (this report's cover photo is an artist's representation of just such an event).

As the largest all metal asteroid in the solar system it would be the most likely core candidate. Geologists would like to find out more about (16) Psyche's properties. Measurements of its potential magnetic field would help determine if it were once a melted core, or perhaps, if no field was measured, it could be indicative of (16) Psyche's origin being earlier in the solar system's formation and closer to the Sun. A detailed analysis of its composition would help to confirm or inform theories of its origin. Imaging of its surface features can show the crater morphology, giving details to (16) Psyche's bulk properties. Details on its physical shape will give clues as to where (16) Psyche came from.

### 1.1.2 Vehicle Overview

At a high level for context, the Psyche Mission explores for the first time, a world of not ice or rock, but of metal. The main purpose of determining whether 16 Psyche is the remnant partial core of a planetesimal - a small world that is the first building block of a planet, identify how old the asteroid is, whether it formed in conditions similar to Earth's core, and characterize the surface. The discovery of a planetesimal could offer insight into Earth's hidden core.

An additional secondary objective includes demonstrating laser communication by encoding messages on photons. However this is not the focus of the mission and should be considered not critical.

As an introduction to the time frame, the target launch date is set for August 2022 at Kennedy Space Center, Cape Canaveral, Florida. Launched from a SpaceX Falcon Heavy Rocket, the spacecraft is geared to arrive in 2026. The trajectory will include a 21

month operation period, with four staging orbits, each becoming progressively lower in altitude.

In terms of size, with the solar wings deployed, the common reference is “parking a smart car into a tennis court”. Where the spacecraft body is the car and the tennis court is when solar arrays are deployed. True dimensions when the spacecraft deployed including solar panels are 25m x 7.3m; a single’s court is 23.77m x 8.23m.

Launch Mass	2,555 kg
Dry Mass	1400 kg
Payload Mass	70 kg
Power	9.5kW-2.3kW [4]

Table 1: Psyche Basic Stats

## 1.2 Mission Objectives

The Psyche mission is dual purpose. Psyche will determine the character and composition of the 16 Psyche Asteroid as well as demonstrate and test the DSOC, or Deep Space Optical Communications.

The primary science objectives are the following [4]

- A. Determine whether Psyche is a core, or if it is primordial unmelted material.
- B. Determine the relative ages of regions of Psyche’s surface.
- C. Determine whether small metal bodies incorporate the same light elements into the metal phase as are expected in the Earth’s high-pressure core.
- D. Determine whether Psyche was formed under conditions more oxidizing or more reducing than Earth’s core.
- E. Characterize Psyche’s topography.

These science objectives are realized in the information gathered from the science instruments aboard during the orbits around 16 Psyche. Broadly, the instruments will [4]:

- Determine the gravity field
- Determine the magnetic field
- Image and create topographical mappings of the surface
- Determine surface composition

The Psyche mission will use the DSOC (roughly) throughout its first year as a tech demonstration. Psyche does not rely on the DSOC for data readings that further the scientific goals [5]

## 1.3 Customer & Stakeholder Requirements

A number of stakeholders include government agencies, private contractors, universities and taxpayers. Note that with a successful mission, everyone will benefit from gaining a stronger overall knowledge of iron cores. Specifically refer to the following customer & stakeholders below [6][7]:

1) NASA/JPL

Stakeholder Requirements: JPL shall develop radio science instruments, and DSOC (Deep Space Optical Communications)

2) Arizona State University: Public University

Stakeholder Requirements: Shall build Multispectral Imager

3) Maxar Technologies:

Stakeholder Requirements: Shall ensure Mission Psyche is manufactured

4) John Hopkins University: Private University - Applied Physics Lab

Stakeholder Requirements: Shall develop Gamma-Ray and Neutron Spectrometer

5) Technical University of Denmark (DTU): Private University

Stakeholder Requirements: Shall co-develop the magnetometer

6) MIT: Private University

Stakeholder Requirements: Shall co-develop the magnetometer

7) United States Taxpayers:

Stakeholder Requirements: Shall contribute tax funding

## 1.4 Concept of Operations

### 1.4.1 Timeline

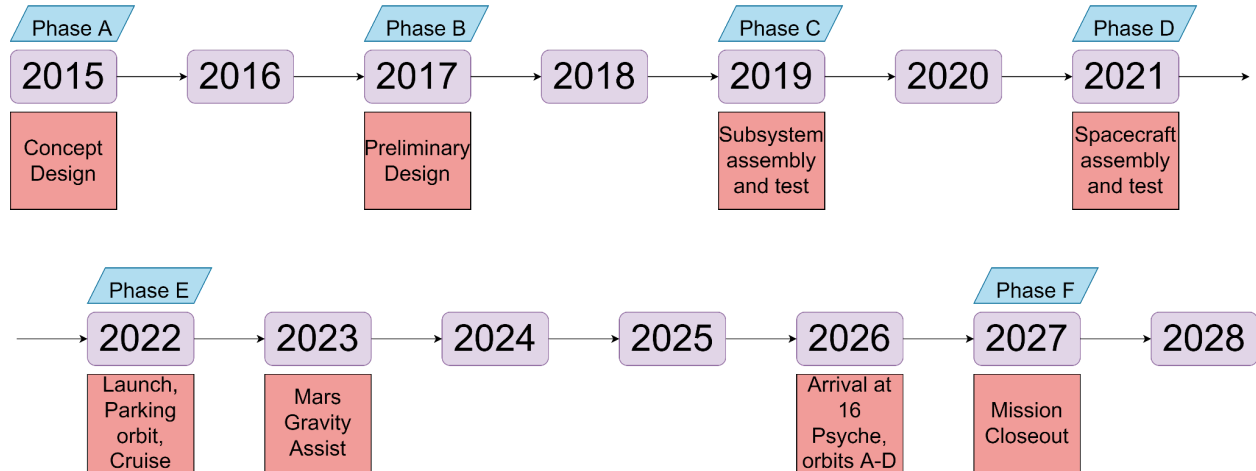


Figure 2: Psyche Mission Timeline

### 1.4.2 Timeline Breakdown

#### Phase A: Concept Study

- September 2015 to December 2016 - team lead by Lindy Elkins-Tanton developed and submitted a thousand page concept study to be reviewed by NASA.

#### Phase B: Preliminary Design of All Instruments and Spacecraft

- January 2017 to May 2019 - science and engineering teams designed the spacecraft and instruments. PDR completed.

#### Phase C: Final Design/Subsystem Fabrication, Assembly, and Test

- May 2019 to January 2021 - instruments begin to be built and bus completed. CDR for Project and Flight Systems completed. Systems Integration Review completed.

#### Phase D: Instrument and Spacecraft Assembly and Test

- January 2021 to July 2022 - spacecraft subsystems are integrated onto bus. Spacecraft undergoes vibration testing, thermal-vacuum testing, electromagnetic interference and compatibility testing, and conducts Operations Readiness Review.
- May 2022 - Psyche ships to launch site
- August 2022 - Launch, initial checkout, cruise to mars

#### Phase E: Cruise, gravity assist, arrival, orbit

- May 2023 - Mars Gravity Assist
- January 2026 to October 2027 - Arrive at 16 Psyche, orbit, and utilize science instruments to complete mission. This occurs in four increasingly smaller orbits

- Orbit A - determine gravity field, determine optimal Orbit B, 56 Days
- Orbit B - topographic surface imagery and mapping, 80 Days
- Orbit C - finish gravity and magnetometry sciences, 100 Days
- Orbit D - use Gamma Ray Neutron Spectrometer to determine surface composition, 100 Days

#### Phase F: Mission Closeout

- November 2027 to August 2028 - Decommission spacecraft

Conops data synthesized from two sources [5][8].

## 1.5 Product Breakdown Structure

### 1.5.0 Flowchart

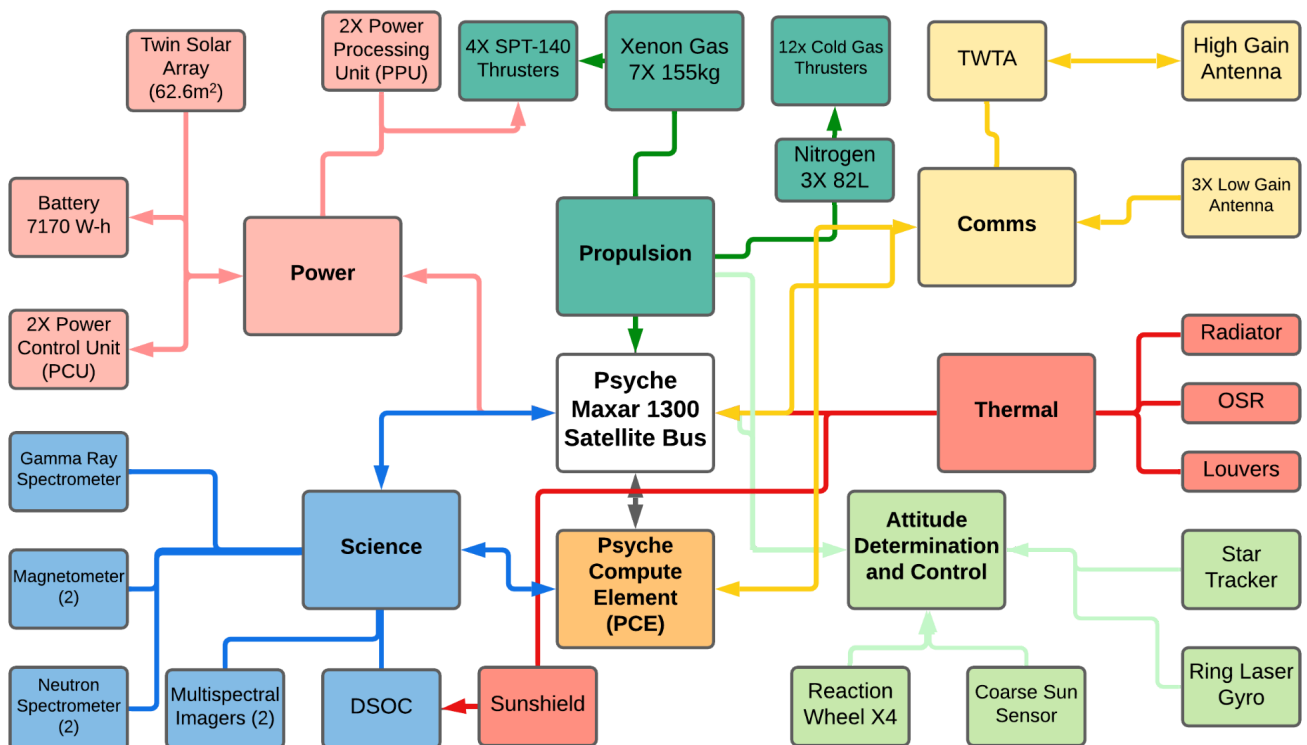


Figure 3: Psyche Product Breakdown Structure

### 1.5.1 Bus

#### 1.5.1.0 Broad Description of subsystems

The Psyche spacecraft can be divided into 7 subsystems, the main bus, power, propulsion, communication, thermal, attitude determination and control, and command

and data handling. Additionally the main purpose of the mission is to carry a payload of scientific instruments in order to study (16) Psyche. A more detailed description of components of these subsystems follows.

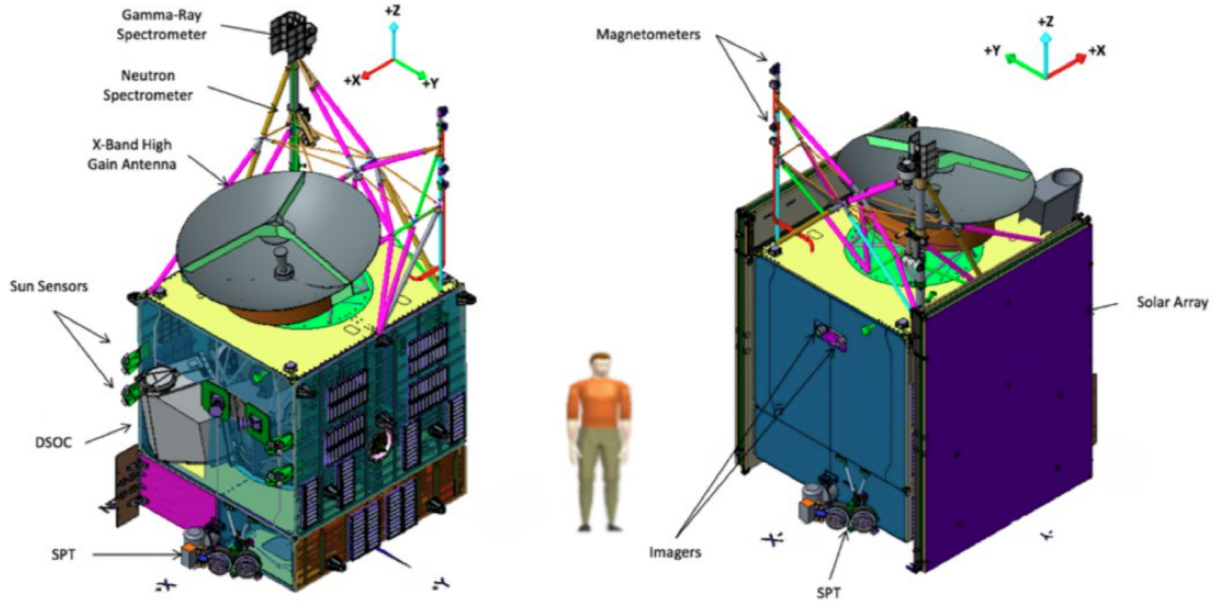


Figure 4: Psyche Spacecraft Overview [4]

#### 1.5.1.1      SSL-1300 Bus

Psyche is built on the SSL-1300 bus produced by Maxar. This proven satellite bus is designed as a fully functional geosynchronous Earth orbit satellite for communication and remote sensing. Customers can implement whatever instruments they need into the payload module, the 1300 can handle all other functions [9]. With the needs of the Psyche mission varying greatly from the typical mission design of the 1300 many components were either removed or replaced with ones that meet the mission requirements [10]. These changes will be noted throughout this product breakdown. The 1300 bus was chosen for its heritage of long life and high power configurations and its proven success utilizing solar electric propulsion.

#### 1.5.1.2      Propulsion

Psyche's propulsion system can be broken down into two main subsystems. Its main thrust is provided by four SPT-140 Hall effect thrusters. Its second system is a network of 12 cold gas thrusters powered by compressed nitrogen.

Hall effect thrusters produce thrust by generating a plasma (in this case from Xenon gas). The plasma is accelerated through an electric field controlled by an applied

magnetic field. The exhaust velocities are very high compared to chemical rockets. The power required is quite high, however, and the thrust produced is in the range of milli-Newton's.

#### 1.5.1.2.1 **SPT-140 Thrusters**

The SPT-140 Hall Thrusters used are manufactured by Maxar. Four of them are integrated into Psyche. Despite having 4 only 1 will ever be firing at a time. Three thrusters will be cycled through during thrusting periods with the fourth intended for redundancy.

These SPT-140s have been tested for use in deep space missions, however Psyche will be the first where they are the primary engine [10]. As the satellite moves farther away from the sun the available power (provided by solar panels) drops. At GEO these thrusters are designed to operate at 4.5 kW, but at 3.3 AU they will be limited to 0.8kW. Testing was completed to verify the characteristics of the thrusters at these lower power levels. A full life test demonstrated 10,371 hours of operation for a single thruster, using 500kg of propellant.

#### 1.5.1.2.2 **Xenon gas in pressure vessels**

The Xenon gas to be ionized for the thrusters is contained in 7 composite overwrapped pressure vessels (COPVs) holding 155kg of xenon each. The max load is expected to be 1085 kg. This mission will utilize the largest amount of xenon of any space mission before it. The xenon is stored at 2700 psi and distributed through a proportional flow controller with variable set points [12].

##### **a. Cold gas thrusters**

12 Cold gas thrusters (CGTs) are placed around the spacecraft. Four are placed on the top (+Z) side of the spacecraft, one in each corner and aimed in either the +X or -X direction. Four more mirror these on the bottom (-Z) side of the spacecraft. The remaining four are also placed on the bottom pointed in the -Z plus + or - Y and/or X direction. [4]. The cold gas thrusters will be used primarily for attitude control where the Hall thrusters aren't able to provide enough thrust or during times of high power consumption. The 1300 bus normally uses the same Xenon used for the Hall thrusters to power the cold gas thrusters, though it was discovered that a new regulator and heating system would need to be designed to use this strategy in this mission. Therefore it was decided to use Nitrogen to power the CGTs.

## b. Nitrogen gas in pressure vessels

Three 82L tanks contain the Nitrogen for the CGT system with a possible total mass of 45.9 kg. Estimated budget for the CGT totals 12.5 kg leaving 33.4 kg available for contingencies and redundancy in case of a tank failure.

### 1.5.1.3 Power

#### a. Dual gimbaled 5 panel solar arrays.

Maxar's 1300 bus is normally fitted with dual 4 panel solar arrays, however it was discovered that these would not provide enough power while at (16) Psyche. An upgraded 5 panel array was configured using SolAero ZTJ triple junction cells. The total active area of the solar arrays is  $62.6 \text{ m}^2$ . This configuration produces over 21 kW while at Earth orbit, where distance to the sun is 1 AU and temperature of the panels will be  $71^\circ\text{C}$ . The spacecraft, however, uses a maximum of 9.5 kW, therefore the extra power will be shunted. Once at (16) Psyche's orbit of 2.4-3.3 AU, the panels will operate at a temperature of  $-105^\circ\text{C}$ . This leads to a maximum production of 2.3 KW. The bulk of the reduction in power will be in reduced power to the SPT-140 thrusters.

#### b. Power Control unit (PCU)

Psyche's power control unit (PCU) coordinates all of the power produced and used on the spacecraft. It takes charge from the solar arrays at 60-105 V. Over 103V power is shunted back to the array. Under 100V the voltage is boosted in the PCU to 100V. The PCU also maintains the charge in the batteries via a bulk charging strategy. 100 V Power is supplied to the power processing units (PPUs) for use in the propulsion system, and to the rest of the spacecraft through a power distribution assembly provided by JPL.

#### c. Power Processing units (PPU)

Psyche uses dual, cross strapped power processing units (PPU). The PPU supplies power to the thrusters as well as the xenon flow controllers (XFC). Each PPU is capable of powering any of the four thrusters or XFCs [13].

#### d. Batteries

Psyche uses a single 7,170 watt-hour Li-Ion battery for use during eclipse times at Psyche as well as when power draw exceeds the output of the solar panels. The battery is composed of a string of 13 cells, with cell shorting devices in case of failure in a cell. A smart battery tray (SBT) monitors the status of each individual cell, maintains optimal

battery temperatures, and provides charge balancing to the cells in order to maximize the life of the battery [13].

#### 1.5.1.4 Communication

Communications are provided through an X-band Small Deep Space Transponder (SDST) and communicates through the Deep Space Network (DSN). The system uses at 100W Traveling Wave Tube Amplifier (TWTA) which enables communication downlink rates of 180kbps using Psyche's high gain antenna (HGA) or a minimum of 10 bps in safe mode using its low gain, omnidirectional low gain antenna [4]. The HGA produces a narrow signal and therefore must be pointed at its intended target in order to communicate. During thrusting operations this will require thrusting to cease and the satellite to be reoriented for communications. During science gathering periods a cadence will be established on regular intervals whereby science will be recorded during a predetermined time interval followed by an equal length time interval to reorient and transmit the data via the HGA. The figure below illustrates the cadence for Psyche's orbit A, its initial orbits around (16) Psyche.

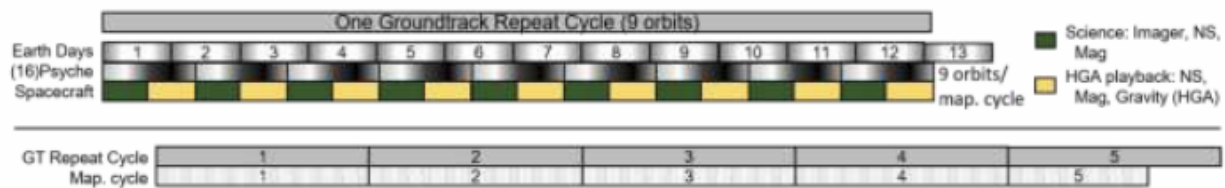


Figure 5: Orbit A Science and Communication Cadence [4]

#### 1.5.1.5 Thermal

The thermal requirements for Psyche are modest compared to a typical Maxar 1300 satellite. Most of the communications equipment has been removed eliminating much of the power draw and therefore heat production. Several modifications have been made to the original 1300 series thermal system. Psyche will be equipped with Maxar's smallest radiator and appropriately sized heat pipes. Passive louvers will be added to maintain optimum temperature inside the spacecraft. They will open when too hot, and close when too cold to hold in radiative energy. [10]. Heaters will help maintain minimum temperatures [4]

Detailed below Psyche is carrying an experimental communication payload, the Deep Space Optical Communication system (DSOC). The optimal conditions for operation of this device is much colder than the rest of the satellite. Therefore it has been placed in an isolated corner of the spacecraft and will be equipped with a sunshade to eliminate radiative heating from the sun.

#### 1.5.1.6 **Guidance, Navigation and Control (GN&C)**

Psyche utilizes an all electric GN&C. Primary control is gained through a combination of its electric propulsion thrusters, its 12 cold gas thrusters, and reaction wheel assemblies (RWAs). Four Honeywell HR 16-100 RWAs are configured in a pyramidal configuration. This allows for continued operation even in the event of a failure of one of the RWAs. RWA momentum unloading can be accomplished during thrust using one of the EP thrusters gimbaled to thrust through the center of mass where small changes in the thrust vector are enough to allow unloading of the RWAs [4]

Attitude determination and navigation are accomplished with a suite of sensors. Psyche includes a star sensor assembly (SSA), and Inertial Reference Unit (IRU), and a “fan” of coarse sun sensors (CSS) [12]. The sun sensor configuration allows for 4-pi steradian views in locating the sun. The IRU is a Honeywell miniature inertial measurement unit (MIMU). The “fan” of 8 CSSs is built by Adcole and offers sensor redundancy. No data is available on the SSA.

#### 1.5.1.7 **Psyche Compute Element**

Avionics, science data management, communication, power distribution are all controlled through the Psyche Compute Element (PCE). The compute element itself is provided by Maxar though the software is provided by JPL [10]. The PCE is a cross-strapped system, allowing for full redundancy. The PCE sends outgoing signals, and receives and decodes incoming signals before passing commands along to the other hardware. The PCE also receives and stores all incoming data from the scientific instruments.

### 1.5.2. Payload

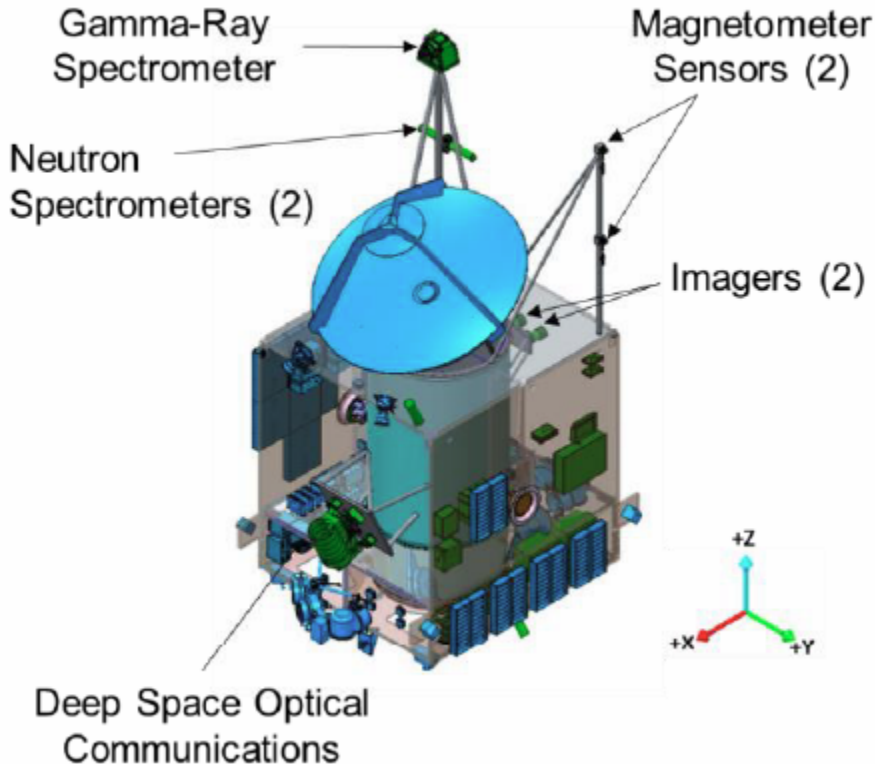


Figure 6: Layout of Psyche's Science Payload [10]

#### 1.5.2.0 Broad Description of Science Payload

The primary purpose of Psyche's payload is to inspect the asteroid (16) psyche. For this purpose it contains imagers, spectrometers, and magnetometers. As a secondary mission psyche is carrying a Deep Space Optical Communications module (DSOC). See figure above for the layout of instruments on Psyche.

#### 1.5.2.1 Multispectral Imagers

Psyche carries dual, redundant multispectral imagers (PMIs) provided by JPL. Their initial mission is to locate (16) Psyche and assist in navigation as the spacecraft approaches. While orbiting (16) Psyche PMIs will provide photographs using both clear and 7 colored filters chosen to assist in determination of surface geology and composition. The PMIs can work in tandem to provide stereo images to aid in developing topographic data [10]. The PMIs are mounted on the -X side of the spacecraft as seen in figure 3

#### 1.5.2.2 Neutron & Gamma Ray Spectrometers

There are 2 neutron spectrometers (NS) and a gamma ray spectrometer (GRS) positioned on a 2 meter boom on the +Z Face of Psyche. Positioned at the end of the boom the GRS measures gamma ray emissions from galactic cosmic rays impacting (16) Psyche's surface. The energies of the emitted gamma rays indicated the elemental makeup of the surface of the asteroid. Similarly the NSs detect "unambiguous measurements of thermal and epithermal neutrons" [10]. The GRS is more sensitive to background energy from the spacecraft and is therefore mounted at the end of the boom, while the NSs are mounted halfway up the boom. Together they are able to detect the presence and location of Iron, Nickel, Silicon, Potassium, Sulfur, Aluminum, Calcium, Thorium, and Uranium.

#### 1.5.2.3 Magnetometer

Two magnetometers will be placed on a separate 2m boom on Psyche's +Z face. One will be mounted at the end of the boom and one at the middle allowing for rejection of meter-scale magnetic fields produced by the spacecraft itself. The magnetometers will search for a magnetic field present in Psyche, and if found it will potentially indicate that Psyche was once the core of a differentiated planetesimal. The devices have a solid heritage though the low temperatures expected at (16) Psyche will necessitate a heating mechanism to be installed on the sensors, proving a potential risk.

#### 1.5.2.4 Deep Space Optical Communications

The DSOC is a piggyback technology demonstration payload to test the viability of using lasers in place of radio communication for high rate deep space operation. The concept might allow downlink data rates of 200 Mbit/s and uplink data rates of 1.6 kbit/s. The experiment will operate during the time that Psyche is traveling between 0.1 AU and 2.0 AU, and will cease operations after that point [10]. The DSOC was built by JPL and is its own independent project with different stakeholders than the main Psyche mission [14].

## Section 2: Background/Heritage

### 2.1. Previous similar spacecraft designs

While the Psyche mission was still in the selection process of the Discovery program, the goal when designing Psyche was to produce a simple, low-risk, highly

implementable mission concept [10]. They accomplished this by using concept operation aspects of the 2015 Dawn Mission, which also orbited large main asteroids at progressively lower altitudes, along with multiple high heritage subsystems. The 2 main high heritage subsystems included Maxar's 1300 bus which was used as the Solar Electric (SEP) Chassis and JPL flight software. Other heritage components included the SPT 140 thrusters, fluxgate magnetometer, multispectral Imagers and gamma ray and neutron spectrometers.

Psyche was originally planned to launch in 2023, but by using an Electrical Power System (EPS) with high heritage from Maxar, this allowed flexibility in the trajectory design [10]. This bus has strong system level heritage through its modular design and has been used in a large number of geostationary communication satellites. Aside from having heritage from the bus, there is also heritage in the thrusters. Maxar has successfully flown over 150 hall thrusters. [16] Additionally, flight heritage of Solar Electric Propulsion (SEP) has been seen in the Dawn mission, a mission to study two of the three known protoplanets of the asteroid belt: Vesta and Ceres.

Psyche's flight software, provided by JPL, has flight heritage from the Mars Curiosity rover. JPL flight software includes guidance and navigation, avionics algorithms, and fault tolerance.

Psyche also includes 3 high heritage instruments. This includes the Fluxgate Magnetometer which has flown in the Magnetospheric Multiscale Mission (MMS) and Insight, the Multispectral imager which has heritage from Mars Science Laboratory Matscam, and Gamma-ray and 2 neutron spectrometers which have heritage from MESSENGER mission. [10]

In conclusion, the integration of these heritage subsystems allowed for the Psyche team to develop a simple, low-risk, highly implementable mission concept.

## **2.2. What's new about your spacecraft compared to previous**

Although there are many subsystems in the Psyche spacecraft that have been flown in previous missions, there are some combinations of these subsystems that are the first. Psyche serves as an experimental spacecraft that combines multiple high heritage systems into 1 completely new system.

Aside from this being the first use of combining these different high heritage systems, it will also be the first time that some of the components in these subsystems are used in deep space. This will be the first time that a Maxar 1300 bus will be flown out into deep

space, beyond geosynchronous orbit, and the first time hall thrusters are used beyond lunar orbit.

This will also be the first time that JPL's high heritage flight software has to interface with Maxar's hardware and bus. JPL will interface with the Maxar hardware through Maxar's Data handling System (DHS). The 2 main interfaces are through Maxar's MBus and a 1553 standard bus. [10]

A new technology, Deep Space Optical Communication (DSOC), will also be tested during the Psyche mission. The DSOC system will use photons as a means of communication instead of traditional radio waves and is expected to increase spacecraft communication performance by a means of 10 to 100 times compared to traditional communication. [15]

## **Section 3: Design to Meet Requirements**

### **3.1. Psyche subsystem requirements**

- at least four levels of flow-down; what is each subsystem required to do?

Figure 7 provides an overall view of all the requirements needed to accomplish this project. In section 3.2, we will further discuss each subsystem that will be modified as a result of our changes.

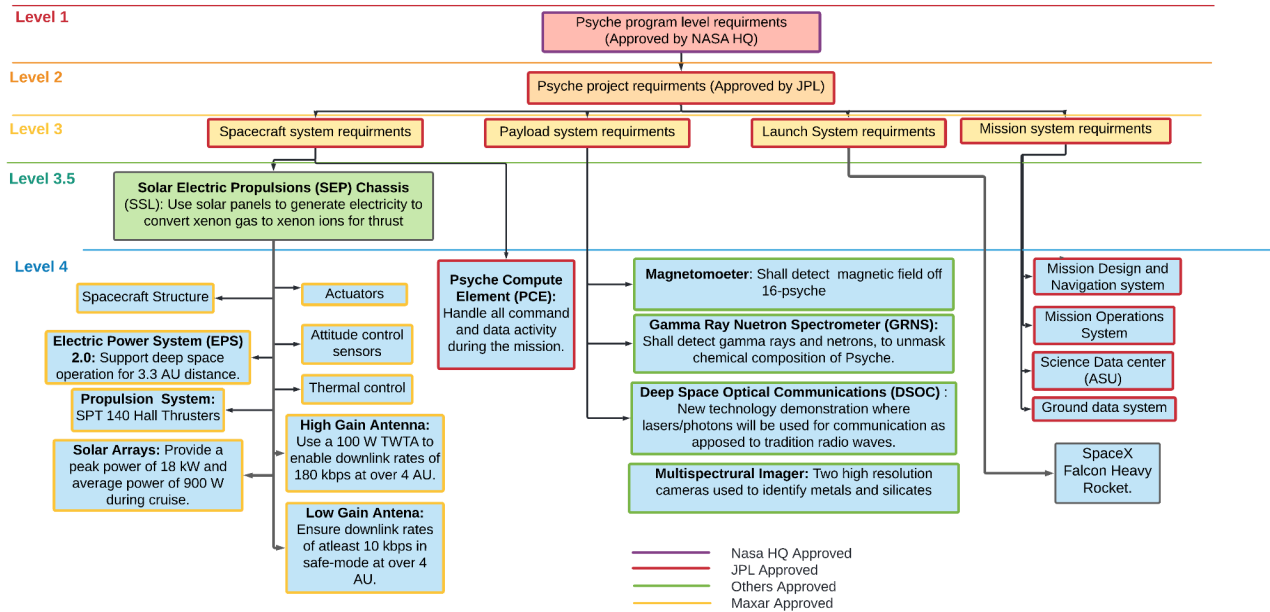


Figure 7: 4-level flow down of Psyche Requirements

## 3.2. Part Modification and Analysis

### 3.2.0 Mission modification motivation

Our goal is to modify the mission performed by the Psyche spacecraft. Specifically we would like to alter the spacecraft to allow it to be used to explore another asteroid after it completes its current mission with (16) Psyche.

In order to accomplish this we plan to increase the available  $\Delta V$  to enable us to leave (16) Psyche orbit and travel to another close but large asteroid. This will involve determining the  $\Delta V$  needed to reach another destination, and then a careful analysis and design to increase the spacecraft  $\Delta V$ . Our team explored several methods for doing this. A short list we came up with included:

- Decreasing the dry mass of the spacecraft
- Increasing the fuel mass of the spacecraft
- Using staging to remove unneeded dry mass (DSOC, empty tanks)
- Finding more efficient engines

From these ideas we developed a modification scheme that includes parts of the first three items. Our proposal includes two physical modifications. The first is to combine the 7 composite overwrapped pressure vessels (COPV) holding the xenon propellant into one larger tank, hoping to save on mass. The second is to use new, lighter, and

more efficient roll out solar arrays (ROSAs) in place of the legacy solar arrays included with the Maxar bus. In both of those cases we propose to maintain the same overall mass by adding the tank mass savings to increase the Xenon propellant and solar array mass savings to increasing the size of the solar arrays, and subsequently to the power produced.

### 3.2.0.1 Propulsion Subsystem Functional Hierarchy

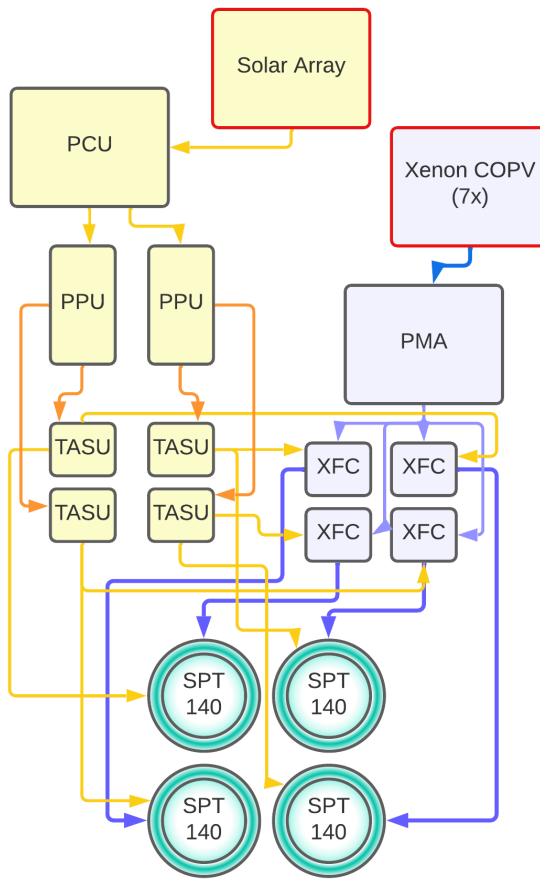


Figure 8: Propulsion Subsystem Hierarchy

A propulsion functional hierarchy diagram is shown in figure 8 above. Our overall goal is to increase  $\Delta V$  through increasing the amount of Xenon propellant we are carrying and increasing the power generated by the solar arrays. Our analyses will include a power and a mass budget analysis. With larger and more efficient solar arrays we will be able to produce more power at (16) Psyche. This power increase will be allocated directly to the thrusters. With increased power the thrusters perform with increased efficiency. The mass budget analysis will be based off the increased initial Xenon mass

available to us as well as our predicted propellant savings due to increased power available to the thrusters.

Our major analysis will be a  $\Delta V$  requirement and orbital maneuvers analysis to determine a target destination and our requirements for getting there. This will require analyzing the requirements for (16) Psyche escape, transferring to a new target, and, if possible, a capture burn around the new target. Alongside that analysis data from the mass and power budget will be used to determine if the required  $\Delta V$  can be met by the reconfigured spacecraft.

### 3.2.0.2 EPS Subsystem Functional Hierarchy

Figure 9 shows the functional hierarchy of the EPS subsystem. The power source requirements, circled in red, are chosen for modification.

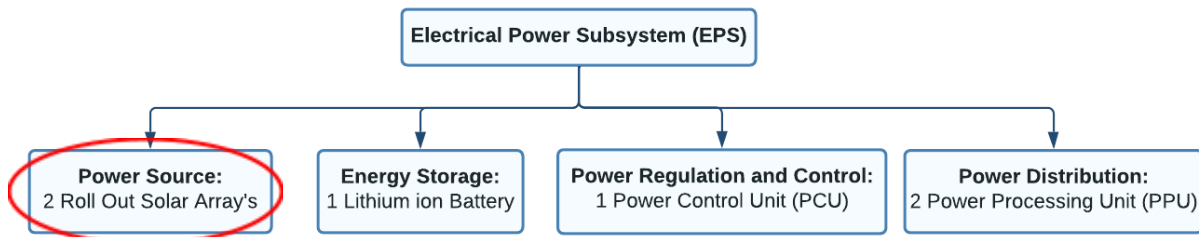


*Figure 9: EPS Subsystem Functional Hierarchy*

The current power source requirements are to provide 2.3 kW of power at 3 AU from the sun (Psyche destination) [11]. Instead, the requirement would change to generate 5 kW of power at 3 AU. A detailed explanation of where this number came from is given in section 3.2.1.

### 3.2.1 New Power Requirements for ROSA

In order to keep all other components the same, while modifying the power source for optimal operation, our maximum power input is dependent on the operating range of the Power Processing Unit (PPU). Table 2 shows the operating range of some SEP performance parameters, including the operating range of the PPU.

Performance <sup>†</sup>	
PPU Input Power	1.0 to 5.0 kW
Predicted Flow Rate	4 to 16 mg/s
Predicted Thrust	50 to 260 mN

<sup>\*</sup> stored in file system onboard the spacecraft  
<sup>†</sup> provided for recurring trajectory analysis

Table 2: Operating range of Performance Parameters [17]

Therefore, in order to deliver the maximum possible power to the thrusters, we need to maintain a minimum power input to the PPU of 5kW.

The current power source produces only 2.3 kW of power at Psyche (3 AU), meaning it does not use the thrusters at full operating capacity.

### 3.2.2 Risks and uncertainties associated with changes

One of the biggest risks we will encounter by making this change, is that we will lose all of the flight heritage that the current rigid solar panels have. The solar panels being used on Psyche have been used in commercial and television satellites, making them effective, reliable, and relatively inexpensive [11].

## 3.3. Trade study to identify ideal design candidates

### 3.3.1 Xenon COPV - MT Aerospace

As stated previously Psyche uses 7 82L COPV tanks to store the 1085 kg of Xenon it carries. The documentation available to the public carries little to no information on the tanks or the connections between them and the initial pressure transducer. From figure 10 below it appears that the tanks are ganged together before reaching the transducer. With this limitation we will rely on the tank mass alone, and assume that the plumbing mass remains the same.

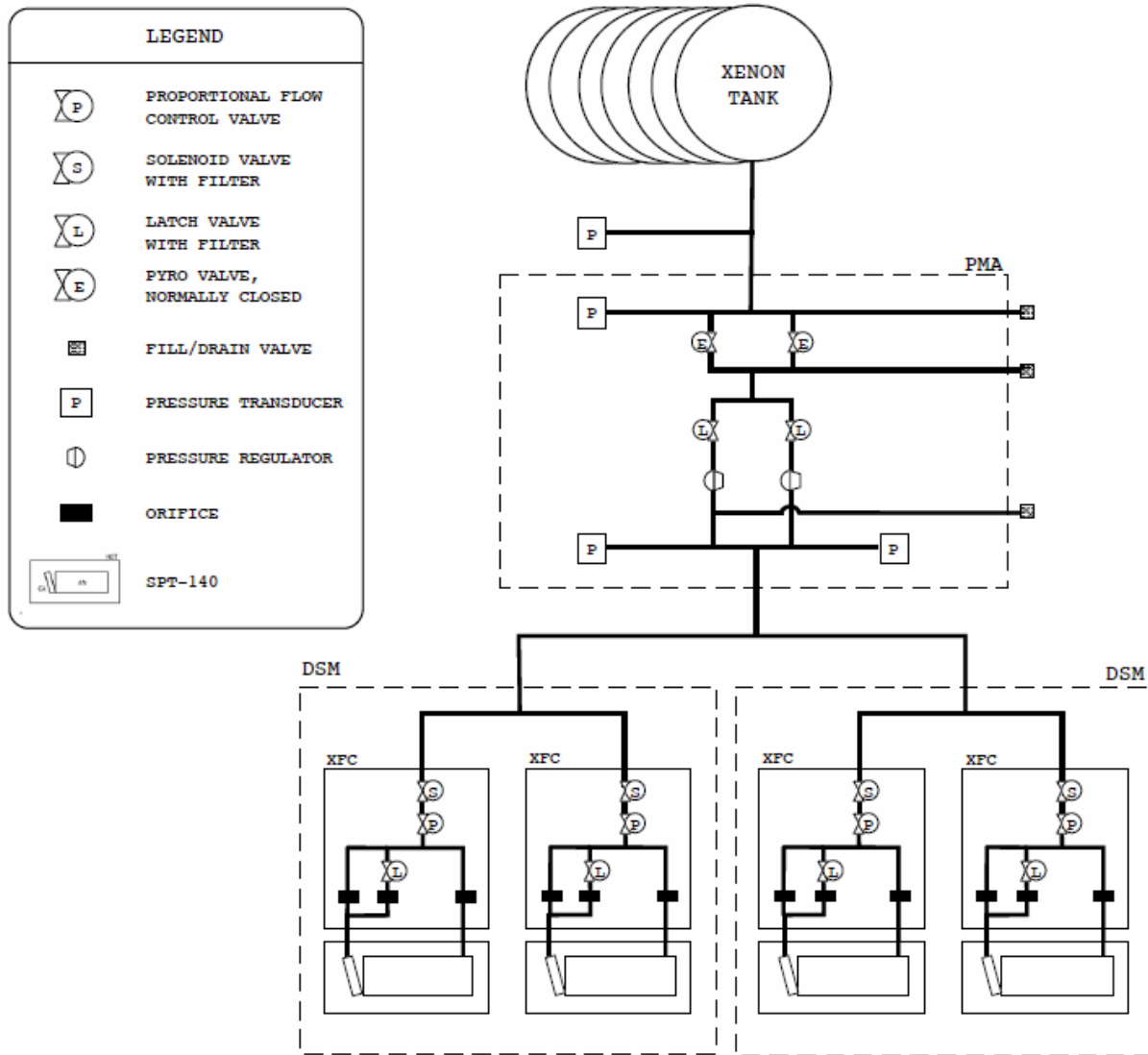


Figure 10: Electric propulsion subsystem pneumatic diagram [17]

Appendix A contains pamphlets from General Dynamics, the provider of the COPVs for Psyche. We identified part number 220165-1 as the candidate for the tanks used. The volume is given as  $5000 \text{ in}^3$ .

$$5000 \text{ in}^3 \cdot 2.54^3 \frac{\text{cm}^3}{\text{in}^3} \cdot \frac{1 \text{ L}}{1000 \text{ cm}^3} = 81.935 \text{ L}$$

This lines up with the 82 L discussed in much of the Psyche literature. The weight for those tanks is listed as 24.5lbs.

$$24.5 \text{ lb} \cdot \frac{1 \text{ kg}}{2.205 \text{ lb}} = 11.11 \text{ kg}$$

Multipled by 7 tanks we get a final tank dry mass of 77.79 kg. The same pamphlet gives us a maximum expected operating pressure (MEOP) of 2700 *psig* ( $1.85 \times 10^7 \text{ Pa}$ ). Using the National Institute of Standards and Technology calculator [20] a density for Xenon at 315 K and  $185 \times 10^5 \text{ Pa}$  was found to be  $1911.9 \frac{\text{kg}}{\text{m}^3}$ . The total volume is  $7 \times 81.935 \text{ L} = 575.545 \text{ L}$  or  $0.575545 \text{ m}^3$ . Multiplied by the Xenon density we calculate a maximum Xenon mass of 1096.56 kg. This is close to the stated maximum 1085 kg Xenon.

A web and literature search for COPV manufacturing specifications led to the discovery of MT Aerospace. They've provided a catalog of spacecraft propellant tanks that they manufacture. Page 13 of this catalog shows and describes their L-XTA/300-900 family of electric propulsion xenon tanks. The catalog indicates that the design is under qualification. It has a volume of 600L, and a dry mass of 68 kg. It also operates at a pressure of 185 bar (2700 psig). Using these conditions a maximum of 1150 kg of Xenon could be stored in this tank as calculated using the density of  $1911.9 \frac{\text{kg}}{\text{m}^3}$ .

The difference in mass between the original tank system and the larger, single tank system is 9.8kg. As stated previously we will use that savings to add an additional 9.8kg of Xenon to the system for a total propellant budget of 1094.8 kg. If needed an additional 55 kg of Xenon could fit into the new tank, though this would increase the overall spacecraft mass.

	Initial Configuration	Proposed Change
Tank Mass (kg)	77.8	68
Tank Volume (L)	575.545	600
Xenon Mass (kg)	1085	<b>1094.8</b>
Total Mass (kg)	1162.8	1162.8

Table 3: Xenon Storage Masses

It is likely that some mass would be saved in the plumbing reducing from 7 tanks to 1. Additionally the mounting system for each option would be different. We weren't able to find any specific information on the mass or configuration of the plumbing or mounting systems except that the 7 tanks were connected through to a single regulator. This suggests that the tanks are ganged together. Therefore we will make the assumption that any potential mass savings will be ignored as they are likely to be minimal and unverifiable.

### 3.3.2 Trade study of ROSA - Deployable Space Systems (Redwire Inc.)

As previously mentioned, we will be swapping the current twin 5 panel solar array with Roll Out Solar Arrays. We chose this modification due to the fact that flexible solar arrays have become more attractive due to higher power density ( $\text{W/m}^3$ ). This means that more power can be processed in a given space or area.

We chose the ROSA's manufactured by Deployable Space Systems (DSS), recently acquired by Redwire inc., because they are the most popular, if not the only, flexible solar arrays currently being tested for deep space travel. These solar arrays have been and are currently being used in the following programs: IROSA (ISS Roll Out Solar Array), Double Asteroid Redirection Test (DART) Mission, Ovzon GEO, and PPE (Power Propulsion Element).

Based on information from the manufacturer's website, there are 2 designs that we can choose for our solar array configuration [18]:

- Single ROSA Wing: A single wing can supply power ranging from 1kW to 30+ kW.



*Figure 11: Single ROSA Wing*

- Mega-ROSA: Consists of multiple ROSA wings arranged on a deployable backbone structure. Can supply power ranging from 20kW to 400+kW.

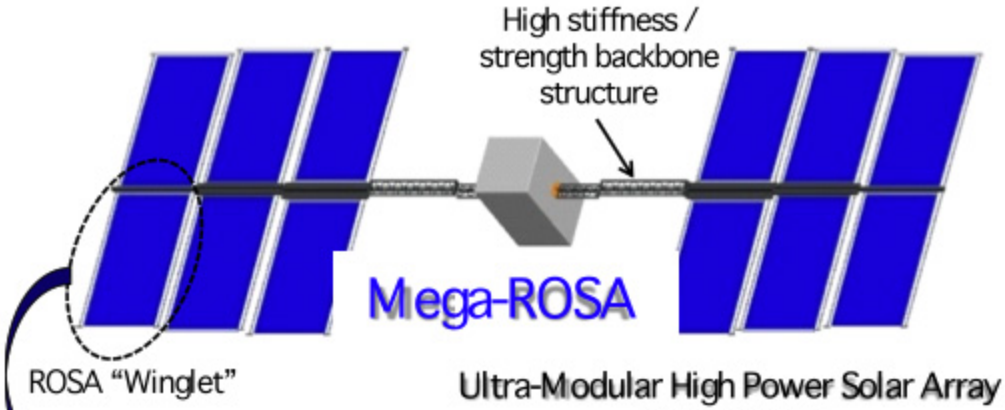


Figure 12: Mega-ROSA Configuration

Another reason that the ROSA was an attractive alternative to rigid solar arrays was due to its scalable design. Redwire advertises ROSA to have a “simple, modular, highly scalable design[18].” This means that we can select the Beginning of Life (BOL) power range needed for our mission, and have a mission specific ROSA produced based on our power needs.

Psyche’s current solar array utilizes ZTJ triple junction solar cells manufactured by SolAero. They offer an efficiency of 29.5% and a mass of  $0.84 \text{ kg/m}^2$ . SolAero also produces an *IMM –  $\alpha$*  solar cell that offers an efficiency of 32.0% and a mass of  $0.49 \text{ kg/m}^2$ . Appendix B contains clips from the spec sheets for each product, provided by SolAero. We will replace the ZTJ cells with the *IMM –  $\alpha$*  cells.

## Section 4: Analyses

### 4.1 Power Budget and Thrust Analysis

#### 4.1.1 Goal of analysis

The goal of this analysis is to determine how power generation will change during the trajectory of the cruise phase. Through research, we have found that the thruster flow rate is dependent on the amount of available power. (insert here how it will affect delta v)

- Determine how our power will change during the trajectory of the cruise phase with the ROSA. (This will determine BOL power, mass & size of ROSA’s)
- Determine how this change will affect the thruster flow rate and if this change will allow us to operate at maximum power for a longer time.

- Determine how the specific impulse will improve throughout the life of the mission.
- Determine how much power we can generate once we arrive at Psyche.

#### 4.1.2. Assumptions, principles, methods used (with refs)

##### 4.1.2.1 Assumptions

For these calculations, we are assuming that all ROSA architectures are perfectly scalable to previous ROSA designs. Because there is no “one size fits all” architecture, the mass, size, and power production of each ROSA is dependent on the program needs. Therefore, we will use previous ROSA numbers for mass, area, and power production and scale them up for our specific spacecraft.

To simplify calculations, the distance away from the sun as a function of days since launch will be approximated to be linear. Figure x shows the original graph, and figure x shows the linear approximation.

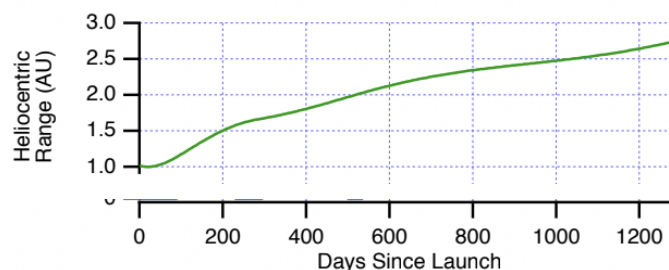


Figure 13: Distance away from the sun as a function of time

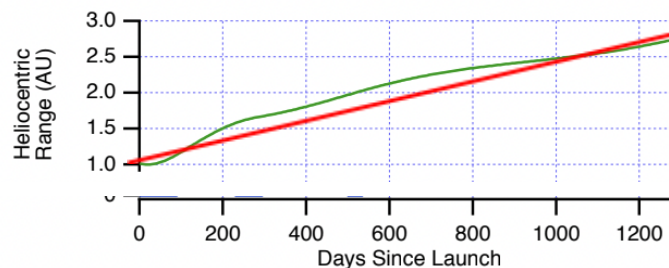


Figure 14: Linear approximation of figure 13

From figure x, and using the equation of a line, we can calculate the distance as a function of time of the spacecraft:

$$y = mx + b \quad 4.1$$

$$r = \left(\frac{2}{1300}\right)x + 1 \quad 4.2$$

Where:

$r$  = Distance away from the sun

$x$  = number of days since launch

Eq 4.2 will be significant during the analysis in section 4.

For simplicity purposes, we will only be conducting the power to trust analysis during the cruise phase of the mission, which is where the power generation increase will be the most significant. This means that all of the science instruments will be turned off, and most of the power generated will go directly to the thrusters.

Our goal is to keep the overall mass of the Psyche spacecraft constant. Mass information has been difficult to come by. Below we compare two different solar cell technologies with different mass densities. Our assumption is that we will be able to keep the mass of the new, lighter solar cells the same as the old cells, by increasing the area. Undoubtedly the mass of the rest of the structure would increase. Our additional assumption is that the mass savings of using a roll out solar array the overall mass will remain the same.

#### 4.1.2.2 Principles

The inverse square law applied to the sun's intensity says that the intensity of the sun is inversely proportional to the square of the distance. The equation that we will be using in our analysis is:

$$I_s = \frac{P_s}{4\pi r^2} \quad 4.3$$

Where:

$I_s$  = Intensity of the sun

$P_s$  = Power of the sun

$r$  = distance away from the sun

At 1 AU this value, known as the Solar Constant, is  $1360.8 \text{ W/m}^2$ .

#### 4.1.3. Math, models, code

##### 4.1.3.1 Current Power Profile

The current power array is  $62.7 \text{ m}^2$ . The power it produces at 1 AU is 21 kW [19]. Their listed efficiency is 29.50% and their mass is  $0.84 \text{ kg/m}^2$ . The total mass of the solar cells is 52.65 kg. Using these values:

$$P_{\text{theoretical}} = 1360.8 \text{ W/m}^2 \cdot 62.7 \text{ m}^2 \cdot 0.2950 = 25,160.50 \text{ W}$$

4.4

As the given power output is given as 21,000 W we can divide the actual value by the theoretical value to determine the inherent degradation for the design.

$$I.D. = 21 \text{ kW} / 25160.5 \text{ kW} = 83\% \quad 4.5$$

Figure 15 shows the range of power as a function of days since launch for the current 10 panel rigid solar arrays. It also shows a side by side comparison of how the power production decreases as we get further away from the sun.

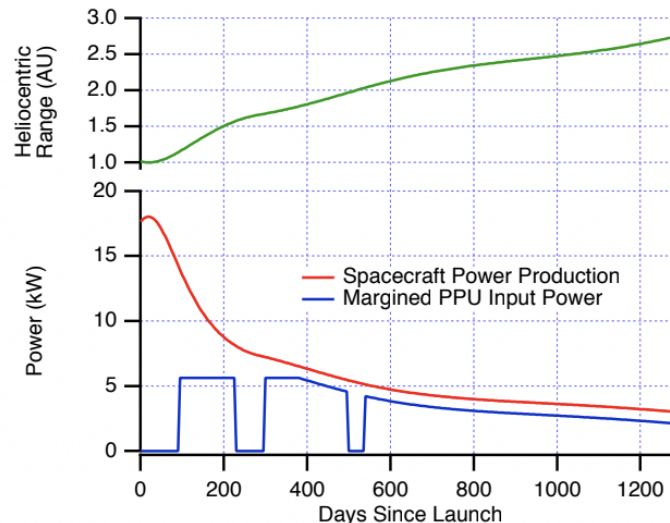


Figure 15: Psyche Cruise Trajectory Power Range [17]

From this graph, we can deduce that the peak power produced is 18kW and drops to 2300 W by the time we reach Psyche. These values are significant because we will compare them with the new peak and average power values estimated to be produced with the new ROSAs. 900W of power is required to power the spacecraft bus [17].

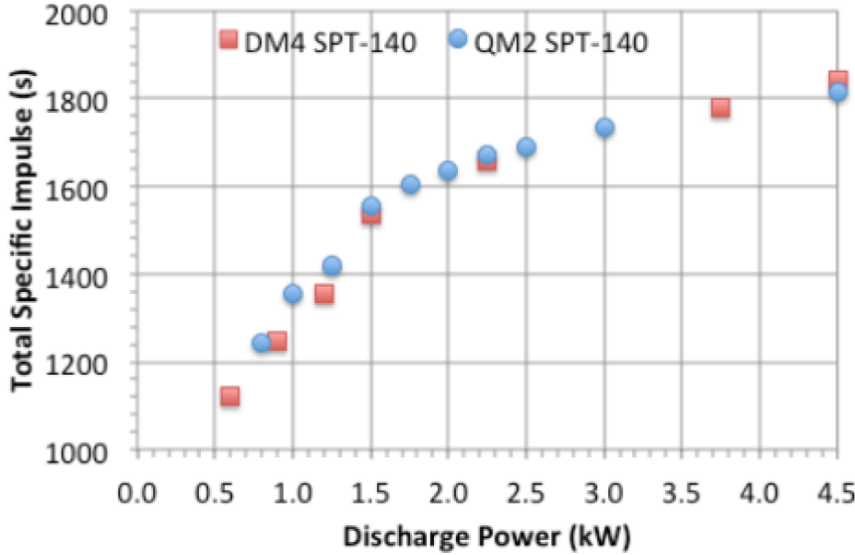


Figure 16: SPT-140 Specific Impulse as a function of Discharge Power

Figure 16 shows the specific impulse of the SPT-140 thrusters as a function of the power supplied to the thruster. At the 1.4 kW available, from the old array, at Psyche the developed specific impulse is around 1450 seconds.

#### 4.1.3.2 New Power Profile

For our new solar arrays we will use the mass of the original cells and calculate a new power budget based off our new, lighter, and more efficient solar cells. Starting with the mass we divide by the density of the new cells.

$$\text{Area} = 52.65 \text{ kg} / 0.49 \text{ kg/m}^2 = 107.445 \text{ m}^2 \quad 4.6$$

From that we can assume the same Inherent Degradation as the original array and calculate power available at 1 AU:

$$P_{1AU} = 1360.8 \text{ W/m}^2 \cdot 107.445 \text{ m}^2 \cdot 0.83 = 38883.68 \text{ W} \quad 4.7$$

Power is inversely proportional to the square of the distance from the Sun. Calculating for power available at Psyche:

$$P_{3AU} = 38833.68 W / (3AU)^2 = 4314.85 W \quad 4.8$$

From the approximately 4.3 kW available we subtract 900 W for Psyche's bus and have 3.4 kW remaining for the thrusters. Referring back to figure 16 above this will correspond to an improved specific impulse of about 1750 seconds [11].

## 4.2 Mass Budget Analysis

Two factors necessitate the need for recalculating the mass budget. With the replacement of the 7 Xenon storage tanks with one larger tank we saved 9.8 kg and added it back as Xenon propellant. With our solar array modifications we increased the power available to us, allowing us to operate the SPT-140 thrusters with more power, developing a higher specific impulse ( $I_{sp}$ ).

The mass budget analysis begins with the propellant mass budget presented in the Psyche PDR. The tables below show the mass of propellant used for each stage of the mission. Using this information and the estimated specific impulse for cruise, 1800 seconds, and for operations at Psyche, 1450 seconds, an estimated  $\Delta V$  can be calculated using the rocket equation:

$$\Delta V = I_{sp} g_0 \ln\left(\frac{m_i}{m_f}\right) \quad 4.9$$

Table 4 shows the  $\Delta V$  calculations, table 5 gives the additional mass information used to make those calculations. The sheet used to make these calculations is linked [here](#) and a copy of it will be included in Appendix B.

Propellant Use Allocation	Xe Mass Used	Total mass remaining	$\Delta V$ required
	kg		m/s
Deterministic Cruise	885	1590.62	8908.348249
Cruise Momentum Management	5	1585.62	57.13836168
Capture to Orbit A	6.4	1579.22	57.53019053
Orbit Transfer: A to B	2.4	1576.82	21.63395051
Orbit Transfer: B to C	1.8	1575.02	16.24708284

Orbit Transfer: C to D	15.8	1559.22	143.4153121
Orbit Maintenance	2.5	1556.72	22.82538023

Table 4:  $\Delta V$  Calculations

	Mass (kg)
Xenon Mass from Above	918.9
Non-Usable Propellant (residuals, leakage, fill error, thruster startup/shutdown, initial checkout)	38.9
Margin: Missed Thrust	35.4
Margin: Thruster Performance Uncertainties	36.8
Total Xenon Mass for propulsion	1030
Additional Extra Xenon Mass	55
Psyche Dry Mass	1470
Total Xe mass	<b>1085</b>
$N_2$ Mass initial	79.3
Total Mass	<b>2634.3</b>

Table 5: Additional Mass Values

The assumption is made that the cruise portion of the mission will be completed with thrusters operating at their peak efficiency of 4.5 kW producing a specific impulse of 1800 seconds. While this is certainly the case for the trip up through the Mars gravity assist it is likely that it isn't true all the way up to Psyche capture. Given more information about the distribution of thrusting throughout the cruise phase it would be possible to prove that some additional mass savings would come from our modifications. These will not be accounted for in this paper though. The propellant mass usage during cruise will remain the same for our modified calculations.

From the calculated  $\Delta V$  new propellant usage values were calculated using the new specific impulse value of 1750 seconds for maneuvers at Psyche. The propellant used to perform these  $\Delta V$  maneuvers will be less as  $\Delta V$  is directly proportional to specific impulse. Table 6 below shows the new mass budget for these maneuvers.

Propellant Use Allocation	$\Delta V$ (m/s)	Xe mass used	Xe Mass Remaining
Capture to Orbit A	57.53019053	5.304694652	1580.315305
Orbit Transfer: A to B	21.63395051	1.990210021	1578.325095
Orbit Transfer: B to C	16.24708284	1.492998294	1576.832097
Orbit Transfer: C to D	143.4153121	13.11780461	1563.714292
Orbit Maintenance	22.82538023	2.077684931	<b>1561.636607</b>

Table 6: New Mass Budget

The remaining Xe mass of 1561.64 kg is 4.92 kg more than in the original mass budget. That amount, combined with the 9.79 kg additional xenon from the COPV swap and the extra 55 kg in the original Xe budget leave us with a mass of 69.71 kg of Xe remaining at the end of the primary mission. With a specific impulse of 1750 s and a dry mass of 1492 kg we can calculate a  $\Delta V$  budget of 783.9 m/s remaining.

## 4.3 Delta V / Orbital Destination

### 4.3.1 Increase Delta V of Psyche to allow Mission Extension

The primary goal of this analysis is to utilize the improvements from our modifications to extend the mission beyond its current end of life. Increasing  $\Delta V$  allows Psyche to explore new places and collect new data, but in order for this data to be worthwhile, the destination has to be chosen carefully.

The issue of destination is solved with the Psyche team's tagline from their Operations Concept, "Maximize Reuse to Minimize Risk." Reusing the entire scientific payload in a similar way to the original Psyche mission minimizes risks that arise from replacement and management of new scientific instruments.

The asteroid 216 Kleopatra is the second largest M-class asteroid in our solar system (the first of which being 16 Psyche [21]). It has an effective radius of  $122 \pm 30$  km and has an albedo of  $0.43 \pm 0.10$ . [22]. Since it is M-class, metal-rich 216 Kleopatra is an ideal destination for the Psyche probe to study.

### 4.3.2. Assumptions, principles, and methods used

Several assumptions were used to calculate the orbital trajectories to 216 Kleopatra. The architecture of the physics utilizes the sphere of influence, patched conic, 2D plane, and instantaneous change in velocity assumptions. This essentially reduces flight to consecutive two body problems and direct changes into new orbits, removing the need to solve complicated differential equations. Smaller assumptions include parallel exit velocity with the asteroid, and that proper timing is chosen such that the end of a transfer coincides with the arrival of the celestial body we are trying to reach.

The principles and equations used in calculating these orbits come directly from Francis J. Hale's Introduction to Spaceflight. The order of operations comes from Marti Sarigul-Klijn's lectures in orbital mechanics. The calculations were carried out using custom functions written for each phase of flight and a MATLAB script to initialize variables and call the functions.

The method of calculation is done in three phases. First, the sun-centric Hohmann transfer is calculated such that the periapsis of the original orbit aligns with one side, and the apoapsis of the destination orbit coincides with the other. The resulting discrepancies in  $\Delta V$  between the points of overlap shows how much velocity you need at the sphere of influence in the escape phase and how much velocity you will have at the sphere of influence at the capture phase. These speeds are used to calculate hyperbolic escape from circular orbit and hyperbolic entry into circular orbit at 16 Psyche and 216 Kleopatra respectively.

### 4.3.3. Math, models, code

There were several parameters given for each asteroid. These are the gravitational parameter  $\mu$ , radius at periapsis  $r_p$ , radius at apoapsis  $r_a$ , semi major axis  $a$ , and orbital eccentricity  $e$  (from JPL's Small-Body Database Lookup). These informed which equations to use.

To begin the mathematics section, it is important to derive one simple equation for concise computations of velocity, the parameter we are most interested in, and to minimize truncation errors. The equation for the energy of a given orbit is given as:

$$E = \frac{-\mu}{2a} \quad 4.10$$

The equation for velocity at any radius  $r$  can be written as:

$$V = \sqrt{2(E + \frac{\mu}{r})} \quad 4.11$$

A simple substitution of energy into the velocity equation reduces the function to values more readily available in this situation. The equation reduced to:

$$V = \sqrt{\mu(\frac{2a-r}{ar})} \quad 4.12$$

For the Sun-centric Hohmann transfer, the velocity at the periapsis and apoapsis are the desired outcomes. Since we defined  $r_{p,Transfer} = r_{p,16}$  and  $r_{a,Transfer} = r_{a,216}$ , we can use these values to find the semi major axis of the transfer orbit:

$$a = \frac{r_a + r_p}{2} \quad 4.13$$

Using the semimajor axis of the transfer orbit and the gravitational parameter of the sun, we can readily find the velocity at the periapsis and apoapsis both using the above equation for velocity. This is then repeated for both the 16 Psyche and 216 Kleopatra orbits.

$$V_{inf,Escape} = |V_{p,16} - V_{p,Transfer}| \quad 4.14$$

$$V_{inf,Capture} = |V_{a,216} - V_{a,Transfer}| \quad 4.15$$

(Note: additional equations and calculations are done to graph the resulting trajectories. These are shown in the code appended to the end of this report but will not be discussed due to time constraints.)

For the Psyche-centric phase of flight, the Oberth maneuver is utilized to figure out how much velocity is needed to leave:

$$V_r = \sqrt{V_{esc,r}^2 + V_{inf}^2} \quad 4.16$$

Where

$$V_{esc} = \sqrt{\frac{2\mu}{r}} \quad 4.17$$

This shows how fast we need to be going from any radius  $r$  in order to escape on a hyperbolic trajectory. Using  $V_{inf,Escape}$  from the Solar-centric calculations allows us to find how fast we need to go such that the resulting velocity enters our desired transfer ellipse. To find  $\Delta V$ , we subtract the Oberth velocity from the circular velocity at orbit D, the last orbit around 16 Psyche. The circular satellite velocity at a given radius can be written as:

$$V_{cs} = \sqrt{\frac{\mu}{r}} \quad 4.18$$

For the capture at 216 Kleopatra, we need to discuss the impact parameter and sphere of influence. Checking the impact parameter with the approach distance  $d$  at the sphere of influence informs you if an incoming object will crash into the celestial body, scrape its surface, or perform a hyperbolic flyby. The equations for the above are as follows:

$$b = r_{planet} \sqrt{1 + \frac{V_{esc}^2}{V_{inf}^2}} \quad 4.19$$

$$d = r_{SOI} \cos(\phi) \quad 4.20$$

$$r_{SOI} = a \left( \frac{m_2}{m_1} \right)^2 \quad 4.21$$

In our case, we choose an approach distance between  $b$  and  $r_{SOI}$  so the Psyche spacecraft will be captured by 216 Kleopatra but will not crash into it. Approach distance is chosen instead of calculated because it is standard practice to correct for elevation angle upon approach.

Calculating the velocity at the periapsis (where firing takes place) is not as straightforward as before since many of the details of the orbit are unknown at this point (besides hyperbolic trajectory). Energy is calculated first, then angular momentum, eccentricity, and semi-major axis. This allows us to solve for the radius of the periapsis and then the velocity of the periapsis. The equations will not be explained but for completion's sake they will be listed below:

$$E = \frac{V^2}{2} - \frac{\mu}{r} \quad 4.22$$

$$H = V_{inf}d \quad 4.23$$

$$e = \sqrt{1 + \frac{2EH^2}{\mu^2}} \quad 4.24$$

$$a = \frac{-\mu}{2E} \quad 4.25$$

$$r_p = a(1 - e) \quad 4.26$$

$$V = \sqrt{\mu(\frac{2a-r}{ar})} \quad 4.27$$

To calculate Time of Flight (TOF), we use a few equations. For an ellipse, dividing the period by 2 allows us to get the TOF for a Hohmann transfer:

$$TOF_{Hohmann} = \pi \sqrt{\frac{a^3}{\mu}} \quad 4.28$$

There are quite a few equations used to get TOF for a hyperbola. Assuming we have true anomaly, eccentricity, and semi major axis, we can get to TOF by plugging in the following:

$$\cosh(F) = \frac{e+\cos(v)}{1+e*\cos(v)} \quad 4.29$$

$$F = \text{arccosh}(\cosh(F)) \quad 4.30$$

$$M = e * \sinh(F) - F \quad 4.31$$

$$TOF = M \sqrt{\frac{a^3}{\mu}} \quad 4.32$$

This gives us the time of flight from the periapsis to the position of the true anomaly. All the above equations are listed and derived in Francis J. Hale's Introduction to Spaceflight.

#### 4.3.4. Results: plots, discussion, confidence, weaknesses

After creating and running the script, the resulting  $\Delta V$  and TOF's are tabulated below:

Orbit Phase	$\Delta V$	TOF
16 Psyche escape from Orbit D	166.8 m/s	22.82 hr
Hohmann Transfer from Psyche to Kleopatra	0 m/s	955.3 days
216 Kleopatra capture to radius of 4,675 km	808.1 m/s	2.734 hr
Entire mission	974.9 m/s	2.620 yr

Table 7:  $\Delta V$  and TOF for (16) Psyche to (216) Kleopatra

The graphs that accompany each stage are also shown below:

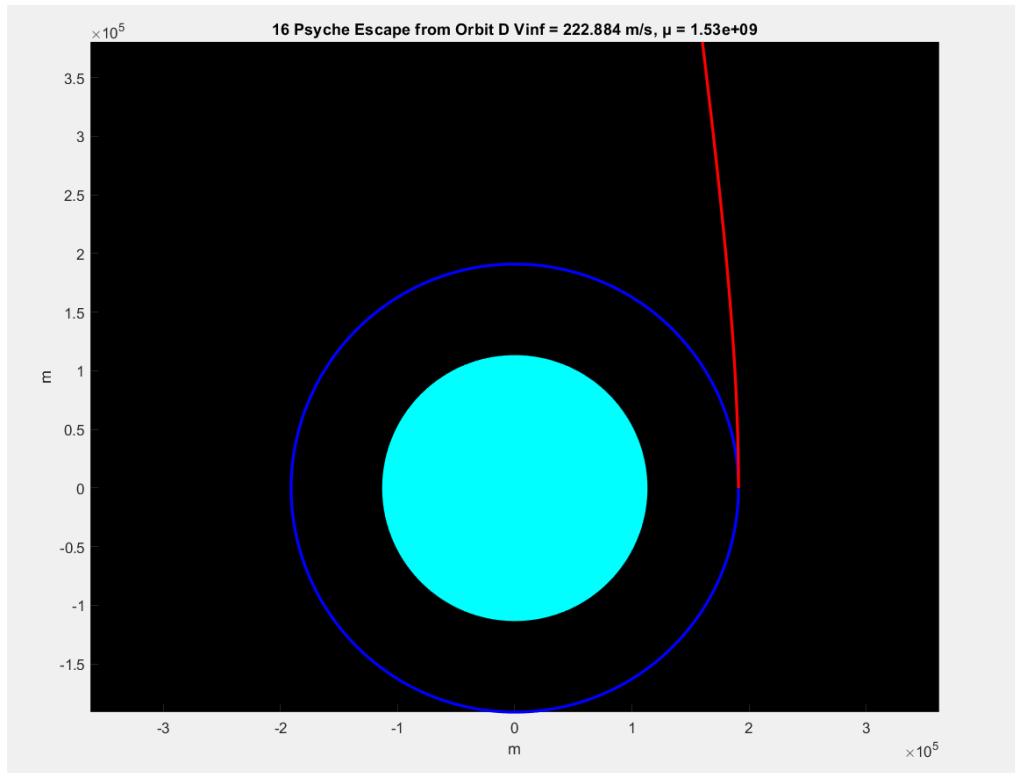


Figure 17: Psyche Escape Trajectory

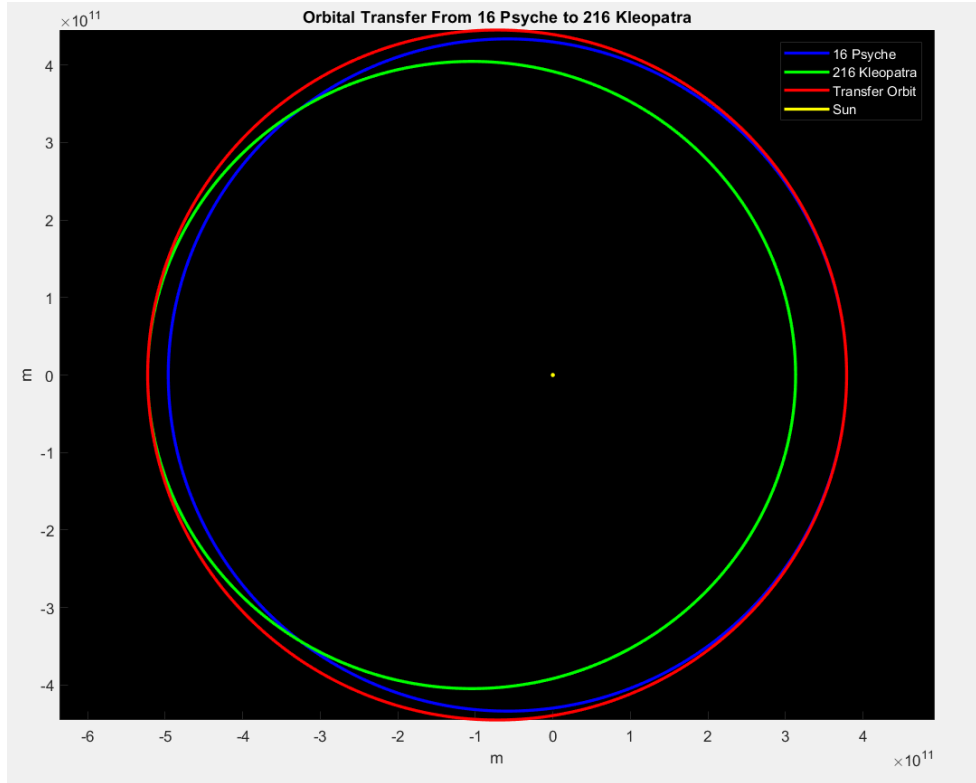


Figure 18: Hohmann Transfer (16) Psyche to (216) Kleopatra

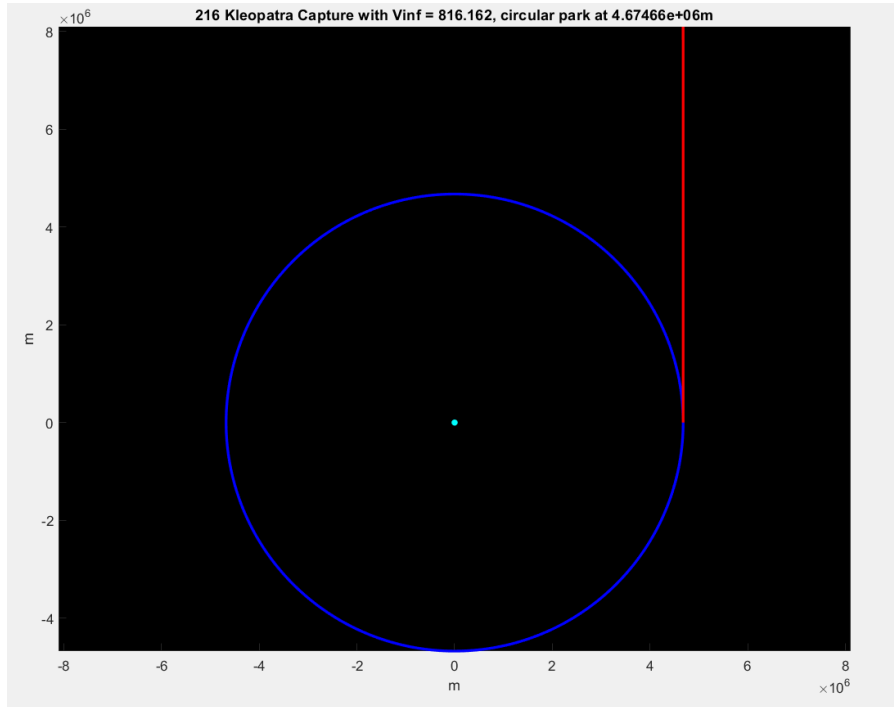


Figure 19: (216) Kleopatra Capture

After the results have been recorded, it is important to discuss the validity of these results and re-assess the accuracy of our assumptions.

The first of the assumptions that should be addressed is the 2D plane assumption. For the 16 Psyche orbit, the angle of inclination is 3.097 degrees [24]. Hale writes that the planets within 3.5 degrees can be assumed coplanar, so we have precedent for this assumption. 216 Kleopatra, on the other hand, has an orbital inclination angle of 13.12 degrees [23], meaning the coplanar assumption is not accurate. More  $\Delta V$  will be required to enter the required plane change.

The second assumption that needs addressing is that of instantaneous change in velocity. With the low thrust high impulse electric propulsion system Psyche uses, change in velocity is about as far from instantaneous as we can get. The numbers calculated are likely of similar magnitude to precise simulations but it is currently unclear if those would produce  $\Delta V$ 's that are higher or lower to our calculated values.

In order to more accurately calculate the  $\Delta V$  of these orbits, differential equations need to be re-derived and solved using numerical analysis. The force balance changes entirely because thrust needs to be accounted for in the force balance. In the equations used thus far, the only force on the spacecraft is that of the planet which is what results in four types of orbits. Allowing for a thrusting force lets us derive the following equations for a two-body assumption:

$$\ddot{x} = \left( \frac{-G\mu x}{r^4} + \frac{F_{thrust,x}}{m_2} \right) \quad 4.33$$

$$\ddot{y} = \left( \frac{-G\mu y}{r^4} + \frac{F_{thrust,y}}{m_2} \right) \quad 4.34$$

From the calculations with the Xenon tanks, thrust is roughly 0.17 N. If we restrict the force of thrust to be perpendicular to the radius, we can get the following expressions for thrust:

$$F_{thrust,x}^2 = \frac{0.17^2}{1 + \left(\frac{x}{y}\right)^2} \quad 4.35$$

$$F_{thrust,y}^2 = \frac{0.17^2}{1 + \left(\frac{y}{x}\right)^2} \quad 4.36$$

These equations are likely incomplete and can be further derived into a more concise form. It is also possible that these equations were derived incorrectly, as previous literature on this topic was not readily available and thus no verification could take place. Performing numerical analyses on these expressions would allow for more accurate thrusting models and thus more accurate  $\Delta V$  while still utilizing the two-body assumption. In an ideal scenario, the initial and boundary conditions for the solar-centric transfer would be as follows:

Initial Conditions	Boundary Conditions
$x_0 = r_{p,16}$	$x_b = -r_{a,216}$
$y_0 = 0$	$y_b = 0$
$\dot{x}_0 = 0$	$\dot{x}_b = 0$
$\dot{y}_0 = V_{p,16}$	$\dot{y}_b = c$

Table 9: Boundary Conditions for Solar-Centric Transfer Orbit

Where  $c$  is a constant to be solved for. Further study needs to be conducted in order to fully realize this mathematical model.

#### 4.3.5. Discussion of how the results are important

The importance of these results exist in the realm of progress. Although our calculated  $\Delta V$  of 974.9 m/s is greater than our budget of 783.9 m/s, the discrepancy is a lot smaller than initial estimations. A difference of two hundred meters per second means that we almost arrived at a parking orbit around 216 Kleopatra. Given more advances in space flight and more space-certified materials, this mission is likely within the realm of possibility.

At present, this difference in  $\Delta V$  results in a flyby of 216 Kleopatra. Because the final burn to enter a circular orbit takes the majority of the  $\Delta V$ , not being able to complete the burn results in a hyperbolic flyby around 216 Kleopatra. During this flyby, the Psyche probe might be able to utilize its multispectral imagers to get a view of Klepatra's two orbiting moons or capture a little bit of gravitational data on its way around. The mission wouldn't be extended as originally intended, but science would still be done with the  $\Delta V$  we have.

## Section 5: Test Plan to Check Analyses

### 5.1. Tests that have been accomplished and create influence

By leaning toward newer technologic modifications, past development and qualifications pave the way for testing our Spacecraft. Recently the 440L and 910 L-XTA or Large Xenon Tank Assembly has been the focus of tank Technology. Not only does it meet ECSS (European Cooperation for Space Standards) but also achieves compliance while holding the lowest possible mass [26]. These two tanks have been tested, and represent the two families of the large tank era. In this way, the idea is to mimic tests for such standards for the 600L tank implemented in the Psyche Spacecraft. Another lead on what to take a look at while testing was the ARTES 33 Mars Sample RTN mission [25]. ARTES 33 is an advanced research group that strives to provide an efficient framework for the Industry-Generated Public/Private Partner (PPP) Research Groups. In fact, Electra was the first PPP that contributed to flight heritage and more credible/representative environments. Unfortunately, there are not many public resources that decide the framework of testing ARTES 33 uses. So that concludes for the 600L Xenon Tank for Psyche, the test consists of meeting ECSS compliance.

### 5.2. Tests that will be executed based on Requirement

While not much was found in existing tests for Roll Out Solar Arrays, the direction taken is that passing structural functionality tests will be required regardless. The tests therefore will cover structural qualification tests for prototypes since both alter the structure. But before structural tests, an electrical test will be performed.

To reiterate, the goal in mind is mission extension, which relies heavily on increasing delta V. Principles that can help achieve increased delta V include the following requirement: By attempting to replace the commercialized 7 COPV tanks with a larger one, the tank must hold 1094kg of propellant and pass ECSS durability tests; Secondly, by attempting to replace the rigid solar panel arrays with ROSAs, the spacecraft must produce 4.3kW of power at end of life. Deriving further, a golden reference will be obtained by performing the electrical functionality tests. In summary, the spacecraft's solar arrays will be connected to a voltmeter. Then the solar arrays will be exposed to artificial sunlight as closely as mathematically modeled concluding a voltmeter reading.

After this step is complete, the spacecraft as a whole will be subjected to the following ECCS tests: Physical properties such as static load tests, pressure, leakage, vibrational, shock, thermal, and microgravity testing [25]. With new mass properties such as mass,

center of mass, and moment of inertia, tests like static load mass help define how the spacecraft can be controlled through ADCS. Although the focus will be the vibrational testing and leak/pressure testing as they hold the largest impact based on our modifications to the spacecraft. Vibrational testing is priority because of the change in resonance frequency to the overall system. The testing unit will be mounted to a table in launch orientation and held stiff enough to prevent anti-resonance generation. There's three types of vibrational tests that the spacecraft will be subjected to: random, sinusoidal, and transient. For the random tests, a Gaussian random excitation(s) will be applied to the base of the adapter in three orthogonal directions with cycle time being 2 minutes per axis. The sinusoidal test will have a sweep rate of 2 octaves per minute and will be the focal point to testing against unplanned resonant frequencies [25]. And lastly, for transient tests, any mathematical modeled frequencies based on the space vehicle launcher should be applied.

Taking a closer look at the tank modification, three tests will also be the focus. The three tests within a similar family of tests are leak, pressure, and LBB (Leak Before Burst). Withstanding the launch environment and high vibrations is vital to the mission. Leak testing will be performed holding the maximum design pressure for 20 minutes. For the pressure testing on a QM (qualification model) the tank will hold 150% of the maximum design pressure for 5 minutes [25]. Note that LBBs framework comes from the Helium High Pressure Vessel Program.

### 5.3. Shortcomings of ground-based testing

In terms of short-comings of ground testing, one item that comes to mind is the artificial lighting for testing the solar arrays. Determining the light source to replicate the sunlight is a unique problem because of the disparity amongst the scientific community's ability to estimate energy levels given a large distance away from Earth's orbit. Another variable that places this test to be a shortcoming of ground based testing is the accurate estimate availability of the light source that actually hits the solar array. To date, scientists have considered two types of sources for these tests: steady state such as filtered xenon or dichroic filtered tungsten and pulsed-type long-arc xenon flash lamps.

The significant impacts that will occur if the Psyche spacecraft fails tests will result in a trade study of the new parts modified. In any sense, failed tests will be tested again with the same conditions. If proven to fail again, options are either to revert to the old design or standardize the part modified even more so. For example, replacing a custom 600L for Psyche SC with an already flight-proven 440L tank.

## Section 6: Conclusion/Discussion

While the proposed changes to Psyche did not allow for the mission to be extended to include orbiting 216 Kleopatra, we were able to demonstrate the ability to escape Psyche and propel through the region of the asteroid belt. It is likely that we would be able to do a flyby of 216 Kleopatra and combine the data from that metal asteroid with what we learned about 16 Psyche.

One additional analysis that was left until now involves the 600L COPV that we swapped out for. In section 3.3.1 it was pointed out that the 1094.8 kg of Xenon fit in the tank with enough room to allow for an additional 55kg (on top of the 55kg included in the original 1085 kg budget). If we calculate adding that mass at the beginning of the mission and recalculating all the thrusting from cruise through orbit D we end up with 132.1 kg of Xe remaining at the end of the primary mission. This would allow for a  $\Delta V$  of 1463.8 m/s. That may actually be enough to escape, transfer, and orbit 216 Kleopatra.

## References

- [1] In Depth | 16 Psyche, *NASA Science Solar System Exploration*, NASA, 2 December 2021,  
<https://solarsystem.nasa.gov/asteroids-comets-and-meteors/asteroids/16-psyche/in-depth/>
- [2] Elkins-Tanton, Linda T. "Asteroid 16 Psyche: NASA's 14th Discovery Mission." *Elements*, vol. 14, no. 1, 2018, pp. 68–68., <https://doi.org/10.2138/gselements.14.1.68>.
- [3] Elkins-Tanton, L. T., et al. "Observations, Meteorites, and Models: A Preflight Assessment of the Composition and Formation of (16) Psyche." *Journal of Geophysical Research: Planets*, vol. 125, no. 3, 2020, <https://doi.org/10.1029/2019je006296>.
- [4] Oh, David Y., et al. "Development of the Psyche Mission for NASA's Discovery Program.", 35th IEPC International Electric Propulsion Conference, 2017
- [5] Polanskey, Carol A., et al. "Psyche Science Operations Concept: Maximize Reuse to Minimize Risk." 2018 SpaceOps Conference, 25 May 2018, 10.2514/6.2018-2703. Accessed 18 Feb. 2022.
- [6] "Psyche Mission | a Mission to a Metal World." Psyche Mission, n.d.,  
<https://psyche.asu.edu/>. Accessed 18 February 2022.
- [7] "Psyche". NASA Jet Propulsion Laboratory (JPL), n.d.,  
<https://www.jpl.nasa.gov/missions/psyche/>. Accessed 17 February 2022.
- [8] "Psyche Mission Timeline | Psyche Mission - A Mission to a Metal World." Psyche Mission, 7 Oct. 2020, [psyche.asu.edu/timeline](https://psyche.asu.edu/timeline).
- [9] *Maxar 1300-Class Spacecraft Bus for RSDO Applications*, Maxar, October 2020,  
[https://rsdo.gsfc.nasa.gov/images/catalog-rapidIV/Maxar\\_1300\\_Data\\_sheet-Rapid\\_IV.pdf](https://rsdo.gsfc.nasa.gov/images/catalog-rapidIV/Maxar_1300_Data_sheet-Rapid_IV.pdf)
- [10] Hart, William, et al. "Overview of the Spacecraft Design for the Psyche Mission Concept." 2018 IEEE Aerospace Conference, 2018, <https://doi.org/10.1109/aero.2018.8396444>.
- [11] Garner, Charles E., et al. "Low-Power Operation and Plasma Characterization of a Qualification Model SPT-140 Hall Thruster." 51st AIAA/SAE/ASEE Joint Propulsion Conference, 2015, <https://doi.org/10.2514/6.2015-3720>.
- [13] Delgado, Jorge J., et al. "Adaptability of the SSL SPT-140 Subsystem for Use on a NASA Discovery Class Missions: Psyche." 52nd AIAA/SAE/ASEE Joint Propulsion Conference, 2016, <https://doi.org/10.2514/6.2016-4542>.

- [14] Hart, William, et al. "Requirements Development and Management on the Psyche Project." *2019 IEEE Aerospace Conference*, 2019, <https://doi.org/10.1109/aero.2019.8741897>.
- [15] Monaghan, Heather. "Psyche and DSOC: 2022." NASA, NASA, 27 Mar. 2018, <https://www.nasa.gov/directorates/heo/scan/opticalcommunications/psyche-dsoc/>.
- [16] Snyder, John S., et al. "Electric Propulsion for the Psyche Mission: Development Activities and Status." *AIAA Propulsion and Energy 2020 Forum*. 2020.
- [17] Snyder, John S., et al. "Electric Propulsion for the Psyche Mission: One Year to Launch." *AIAA Propulsion and Energy 2021 Forum*, 2021, <https://doi.org/10.2514/6.2021-3426>.
- [18] "Roll out Solar Array (Rosa)." *Redwire Space*, <https://redwirespace.com/products/rosa/>.
- [19] Oh, David Y., et al. "Development of the Psyche Mission for NASA's Discovery Program.", 36th IEPC International Electric Propulsion Conference, 2019
- [20] Xenon, National Institute of Standards and Technology, <https://webbook.nist.gov/cgi/cbook.cgi?Name=xenon&Units=SI>.
- [21] "M-Type Asteroids | Facts, Information, History & Definition." The Nine Planets, 5 Mar. 2020, [nineplanets.org/m-type-asteroids/](https://nineplanets.org/m-type-asteroids/).
- [22] Shepard, Michael K., et al. "A Revised Shape Model of Asteroid (216) Kleopatra." *Icarus*, vol. 311, Sept. 2018, pp. 197–209, [echo.jpl.nasa.gov/asteroids/shepard.etal.2018.kleopatra.pdf](https://echo.jpl.nasa.gov/asteroids/shepard.etal.2018.kleopatra.pdf), 10.1016/j.icarus.2018.04.002. Accessed 18 Mar. 2022.
- [23] "Small-Body Database Lookup." [Ssd.jpl.nasa.gov, ssd.jpl.nasa.gov/tools/sbdb\\_lookup.html#/?sstr=216%20kleopatra](https://ssd.jpl.nasa.gov/ssl/lookup.html#/?sstr=216%20kleopatra). Accessed 18 Mar. 2022.
- [24] "Small-Body Database Lookup." [Ssd.jpl.nasa.gov, ssd.jpl.nasa.gov/tools/sbdb\\_lookup.html#/?sstr=16%20psyche](https://ssd.jpl.nasa.gov/ssl/lookup.html#/?sstr=16%20psyche). Accessed 18 Mar. 2022.
- [25] Space Engineering Testing ECSS Secretariat ESA-ESTEC Requirements & Standards Division. 2002.
- [26] "L-XTA – Large Xenon Tank Assembly." Esa.int, 2021, [artes.esa.int/projects/lxta-%E2%80%93-large-xenon-tank-assembly](https://artes.esa.int/projects/lxta-%E2%80%93-large-xenon-tank-assembly). Accessed 18 Mar. 2022.

## Appendix A: COPV Manufacturer Information

### COMPOSITE PRESSURE VESSELS

for Spacecraft and Launch Vehicles

Part Number	Minimum Volume (in³)	DIMENSIONS	PRESSURES (psig)		Maximum Weight (lbs)*
			MEOP	Minimum Burst	
220148-1	220	5.76 x 14.33	8,500	21,250	5.3
220130-1	260	5.0 x 18.03	3,750	11,700	3.5
220147-1	300	5.76 x 17.8	8,500	21,250	6.55
220135-1	340	6.63 x 14.45	4,000	8,000	4.5
220063	490	10.43 x 11.02	3,200	7,150	6
220088-1,3	490	10.3 x 11.02	5,000	10,000	5.3
220088-2	490	10.57 x 11.02	5,000	12,500	6.5
220139-2	490	10.3 x 11.02	3,043	7,608	6.6
220069	541	10.66 x 11.82	4,074	8,148	6.8
220155-1	655	8.5 x 17	2,630	5,260	7.55
220111	880	13.7 x 12.8	5,075	10,150	19
10070890	1,890	17.1 x 14.95	4,000	8,560	17
220074	2,550	18.19 x 19.23	5,000	10,050	33.5
2200153-1	2,550	18.9 x 19.23	5,000	10,050	33.5
220098	3,010	18.71 x 19.18	4,000	6,000	20.05
220121-2	3,010	13.02 x 34.5	4,000	6,000	17.05
220142-2	4,000	12.94 x 37.94	2,700	4,050	20
220145-2	4,000	13.04 x 36.98	4,000	6,000	23.7
220134-1	4,200	12.5 x 42.98	3,500	5,250	22.14
220134-2	4,200	12.65 x 42.98	2,500	7,200	27.6
220165-1	5,000	12.94 x 50.6	2,700	4,050	24.5
10070504-2	6,127	15.2 x 42.3	4,800	7,200	38.4
220086-11	8,181	26.13 x 26.31	4,000	6,000	72.5
10070504-5	9,097	15.2 x 60.4	4,800	7,200	53.1
220132-1	11,500	20 x 47.6	3,000	6,000	75
220122-1	14,212	20.6 x 56.5	3,726	7,500	90.4
10071224-1	14,212	20.6 x 54.5	3,000	7,500	92
220062	18,817	35.77 x 36.86	3,000	12,000	280
10070799	26,093	23.3 x 82.1	6,000	13,500	276
220126-2	31,600	24 x 78.44	300	450	43.4
10070804	42,855	27.3/43 x 66	6,600	13,500	685
10071204	46,138	36 x 63	4,500	10,000	370
220141-1	66,420	40 x 74.5	4,600	6,900	393
10070930	376,000	90 x 78	850	1,800	1,240

\*Weight based on specification, actual value may be lower.

**GENERAL DYNAMICS**  
Ordnance and Tactical Systems

11399 16th Court N. - Suite 200 - St. Petersburg, FL 33716 - (727) 578-8100 - www.gd-ots.com - Approved for public release 09/2009  
Lincoln Operations - 4300 Industrial Avenue - Lincoln, NE 68504 - (402) 464-8211 - gdbdevlincoln@gd-ots.com

07/2014

Figure A1: General Dynamics COPV data (current Psyche design)

**L-XTA / 300-900 Family**

Xenon Tank – Electric Propulsion (EP)

**HERITAGE** under Qualification

<b>FLUIDS</b>	Xenon	
<b>MATERIALS</b>	Shell	Ti-6Al-4V
	Tube	Ti-3Al-2.5V
	Overwrapped	Epoxy-based CFRP / T800
<b>MOUNTING INTERFACE</b>	equatorial skirt	

<b>TOTAL VOLUME</b>	600 - 900 l	36.614 - 54.921 in <sup>3</sup>
<b>TEMPERATURE RANGE</b>	up to 50 °C	up to 122 °F
<b>TANK DRY MASS</b>	68 - 85 kg	149,9 - 187,4 lbs
<b>DIAMETER</b>	1.144 mm	45,04 in
<b>LENGTH</b>	979,3 - 1306 mm	38,56 - 51,42 in
<b>MEOP*</b>	187 bar	2.712 psi
<b>PROOF PRESSURE (x 1,25)</b>	233,8 bar	3.390 psi
<b>BURST PRESSURE (x 1,50)</b>	280,5 bar	4.068 psi
<b>BURST PRESSURE TESTED</b>	bar	psi

**FOR ELECTRA & NEOSAT/  
SPACEBUS-NEO PLATFORMS**

\* Maximum Expected Operating Pressure

Sales Contact: Mr. Rolf Pietschmann & Mr. Markus Staudt – e-mail: [spacecraft-tanks@mt-aerospace.de](mailto:spacecraft-tanks@mt-aerospace.de)

13

Figure A2: MT Aerospace - Xenon EP Tank data

## Appendix B: Solar Cell Data



DATASHEET  
APRIL 2018

**The World Leader in  
Space Power Solutions**

*Over 3.5 million flight solar cells delivered!*



### ZTJ Space Solar Cell

3rd Generation Triple-Junction Solar Cell for Space Applications



**29.5%**  
**Minimum Average Efficiency**

Space Qualified & Characterized to the  
AIAA-S111-2005 & AIAA-S112-2005 Standards

#### FEATURES & CHARACTERISTICS

- 3rd generation triple-junction (ZTJ) InGaP/InGaAs/Ge Solar Cells with n-on-p polarity
- Solar cell mass of 84 mg/cm<sup>2</sup>
- Fully space-qualified with proven large volume manufacturing and flight heritage
- Excellent radiation resistance with P/Po = 0.90 @ 1-MeV, 5E14 e/cm<sup>2</sup> fluence
- Compatible with corner-mounted silicon bypass diode for individual cell reverse bias protection
- Excellent mechanical strength for reduced attrition during assembly and laydown
- Weldable or solderable contacts
- Custom sizes available
- Available as a Coverglass Interconnected Cell (CIC) for integration onto solar panels

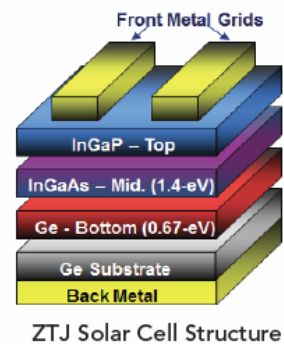


Figure B1: SolAero ZTJ Solar Cells, Original Solar Cells on Psyche Spacecraft



PRELIMINARY DATASHEET  
APRIL 2018

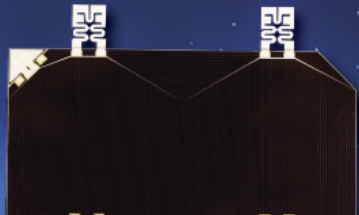
**The World Leader in  
Space Power Solutions**

*Over 3.5 million flight solar cells delivered!*



## IMM- $\alpha$ Space Solar Cell

Highest Efficiency Space Solar Cell in Production



IMM- $\alpha$  CIC  
(Coverglass Interconnected Cell)

**32.0%**  
**Minimum Average Efficiency**

Space Qualification & Characterization to the  
AIAA-S111-2014 standards in progress

### FEATURES & CHARACTERISTICS

- Inverted metamorphic n-on-p solar cell
- 180  $\mu\text{m}$  thickness on rigid carrier substrate
- Solar cell mass of 49 mg/cm<sup>2</sup> which represents a 42% reduction as compared to the ZTJ solar cell
- Radiation hardened design @ 1-MeV, 1E15 e-/cm<sup>2</sup> fluence P/Po = 0.87 (ECSS post-radiation annealing)
- ~3% absolute remaining factor advantage versus ZTJ in charged proton environments with proton fluences equivalent to ~5e14 e-/cm<sup>2</sup> to 1e15 e-/cm<sup>2</sup>, 1-MeV electrons
- Compatible with corner-mounted silicon bypass diode for individual cell reverse bias protection
- Excellent mechanical strength for reduced attrition during assembly and laydown
- Weldable or solderable contacts
- Custom sizes available

Figure B2: SolAero IMM –  $\alpha$  Solar Cells, Replacement Solar Cells for Psyche Spacecraft

## Appendix C: COPV Replacement and $\Delta V$ Calculations

		Table 5. Comparison of key attributes between Psyche and typical SSL GEO comsat						
lb/kg		0.45359237	pounds to kilograms					
l/m		0.001 liters to m <sup>3</sup>						
P		187 Pressure (bar)						
T		315 Kelvin						
Isp max		1850 s						
Isp psyche		1450 s						
Isp Modified		1750 s						
g <sub>0</sub>		9.81 m/s <sup>2</sup>						
Number of Tanks		Initial Conditions Proposed Changes						
Volume of each tank (L)		7	1					
Total Volume (L)		82	600					
Mass of each tank (kg)		574	600					
Total tank mass		111301307	68					
Mass of Xe (kg)		77,791,091.46	1085	1094,791,091	9,791,091.457			
Extra Xe/Mass from COPV Swap								
Usage-Category/Propellant								
Allotment	kg	Total mass remaining	Delta-V required					
Deterministic Cruise		885	1590.62	8908.348249				
Cruise Momentum Management		5	1585.62	57.13636168				
Capture to Orbit A		6.4	1579.22	57.53019053	1580.3115305	5.304694652		
Orbit Transfer: A to B		2.4	1576.82	21.63396561	1578.325095	1.980210021		
Orbit Transfer: B to C		1.8	1575.02	16.24708284	1576.332097	1.492896294		
Orbit Transfer: C to D		15.8	1559.22	143.415121	1563.14292	13.11780461		
Orbit Maintenance		2.5	1556.72	22.82538023	1561.636607	4.916607496	14.707659895	Total increased propellant mass at completion of initial mission
Non-Usable Propellant (residuals, leakage, fill error, thruster startups/shutdown, initial checkout)		38.9					69.707659895	Xe Remaining at primary mission completion
Margin: Missed Thrust		35.4						
Margin: Thruster Performance Uncertainties		36.8	delta V available	783,945.584				
Total 1030.0 kg		1030						
assume cruise uses the same amount of propellant								
Dry Mass kg		1470						
Initial Xe mass kg		1085						
N <sub>2</sub> Mass initial		79.3						
Total Mass		2634.3						

$$\Delta V = I_{sp} g_0 \ln\left(\frac{m_i}{m_f}\right)$$

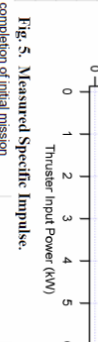


Fig. 5. Measured Specific Impulse.

## Appendix D: Orbital Mechanics Calculations

```
% code written by
% Michael Gunnarson
% as a part of the UC Davis EAE 143 Psyche team:
% Jackie Arroyo Donjuan, Nickolas Loftus, Michael Gunnarson,
Christian Lum.

% Orbital mechanics hand calculations use patched conic sections
to acquire
% rough estimates of transfer from 16 Psyche to 216 Kleopatra.
% Assumes instantaneous impulse and parallel exit velocity
with planet.
% Assumes that timing is chosen so all asteroids will be in
ideal positions
% Uses sphere of influence assumption. Assumes 2D plane

% This code is used to calculate how much delta v we would need to
get from
% 16 Psyche to 216 Kleopatra, both of which are large
metallic asteroids.
% More delta v would be required to perform data maneuvers around
216 % Kleopatra.

clear
format long
clc
```

## Constants

```
% physical and orbital data from Francis J. Hale's Introduction to %
Spaceflight. Psyche data taken from https://ssd.jpl.nasa.gov/tools/
sbdb_lookup.html#/?sstr=16
% 216 Kleopatra data taken from
https://ssd.jpl.nasa.gov/tools/
sbdb_lookup.html#/?sstr=2000216
% 16 denotes 16 psyche, 216 denotes 216 kleopatra

% radius
rEarth = 6.378E6; % m
rMars = 71.40E6; % m
rSun = 696.0E6;
r16 = 226/2*1000; % diameter
r216 = 54.25*1000; % equivalent radius, m, https://
www.sciencedirect.com/science/article/pii/S0019103510004355

% mu
muEarth = 3.986e14; % m^3/s^2
```

```
muMars = 4.297e13; % m^3/s^2
muSun = 1.327E20;
mu16 = 1.53*1000^3; % m^3/s^2

% mass to mu
m216 = 4.64E18; % kg
https://www.sciencedirect.com/science/article/pii/S0019103510004355
G = 6.674E-11; % m^3/kgs^2 from
https://physics.nist.gov/cgi-bin/cuu/Value?bg
mu216 = G*m216;

% semimajor axis
aEarth = 1.000; % AU
aMars = 1.524; % AU
aBelt = 2.06; %
fromhttps://en.wikipedia.org/wiki/Asteroid\_belt a16 =
2.924484673106921; % AU
a216 = 2.793277353255009; % AU

% eccentricity
eEarth = 0.0167;
eMars = 0.0934;
e16 = 0.133926624302819;
e216 = .2507297431057924;

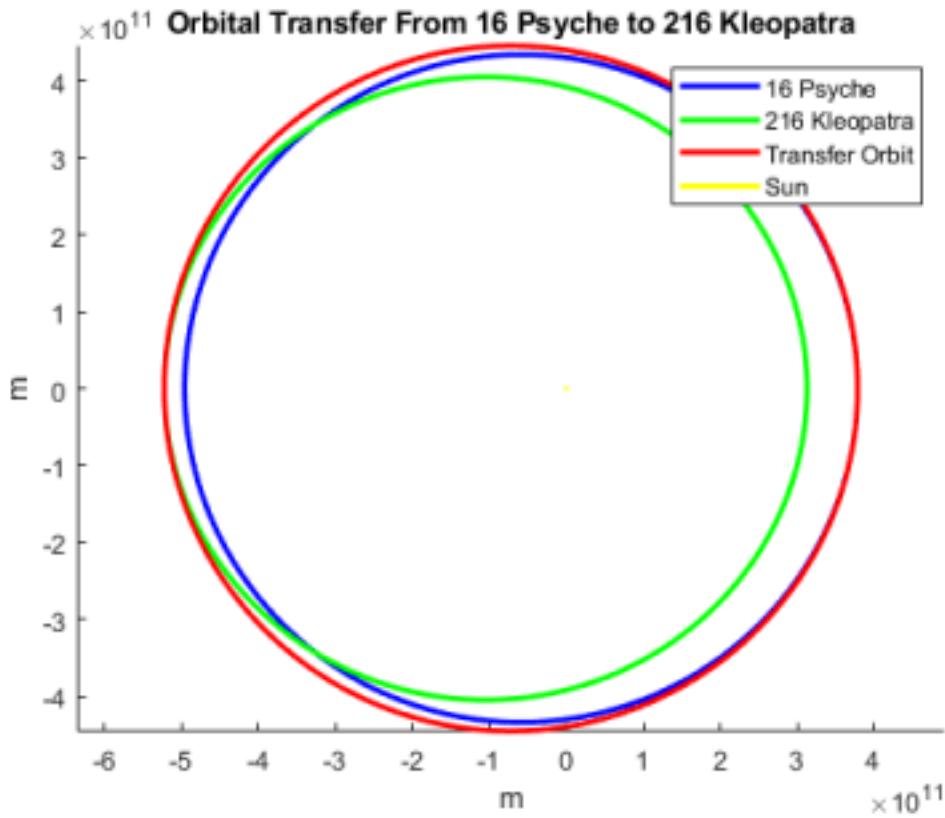
% orbital velocity
velEarth = 29790; % m/s
velMars = 24140; % m/s

% Asteroid Orbits
ra16 = 3.316151033201463; % AU
rp16 = 2.532818313012378; % AU
ra216 = 3.493635066459865; % AU
rp216 = 2.092919640050153; % AU
```

## Solar-Centric Transfer

```
% unit conversions
a16 = AUtoM(a16);
ra16 = AUtoM(ra16);
rp16 = AUtoM(rp16);

a216 = AUtoM(a216);
ra216 = AUtoM(ra216);
rp216 = AUtoM(rp216);
[dv2,dv3,tTsfr,va16,va216,vp16,vp216,vaTsfr] =
transfer(a216,ra216,rp216,e216,a16,ra16,rp16,e16,rSun,muSun);
```

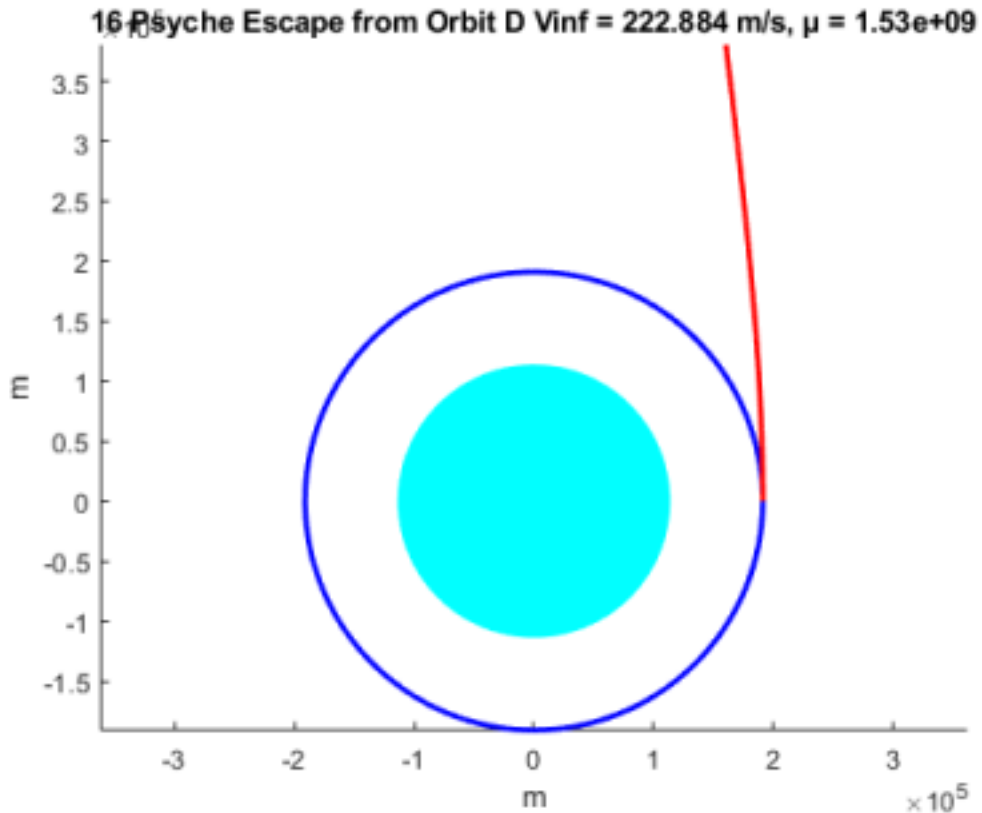


**16**

## Psyche Escape

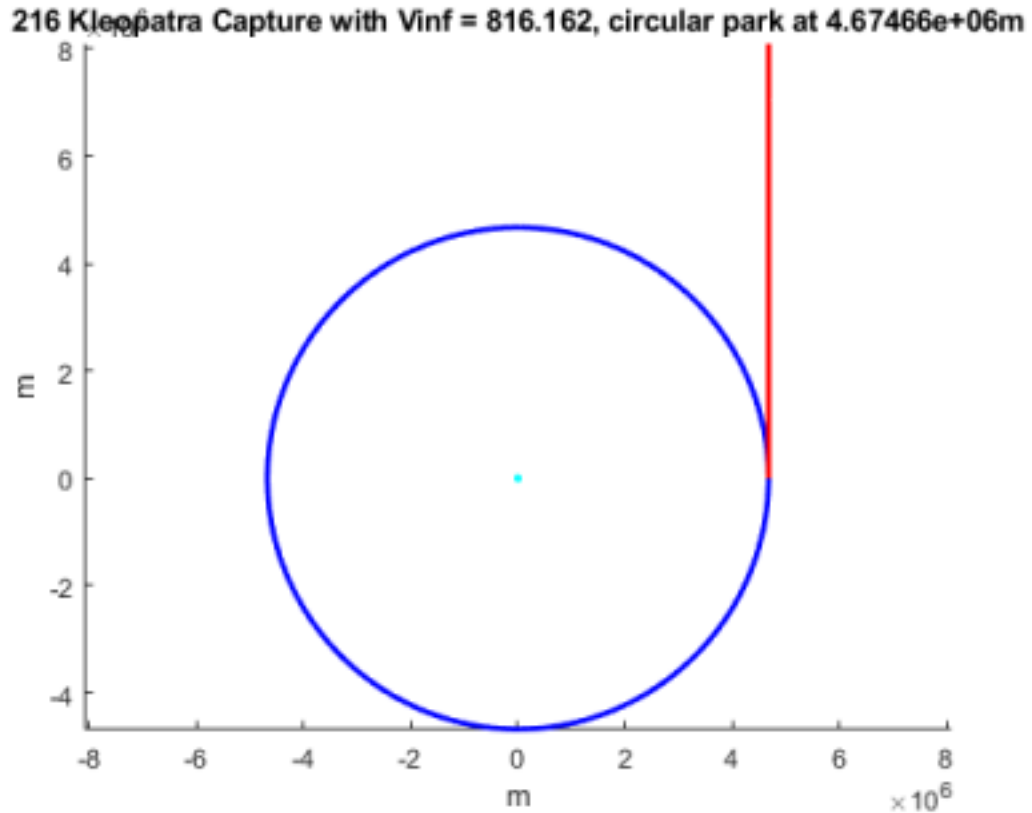
```
vInf = dv2;
rOrbitD = 191E3; % m
% from Psyche Science Operations Concept: Maximize Reuse to
Minimize Risk
```

```
[dv1,tEsc] = escape(mu16,muSun,rOrbitD,vInf,r16,a16);
```



## 216 Kleopatra Capture

```
vInf = abs(vaTsfr-va216);
[dv4,tCap,rp] = capture(mu216,muSun,a216,r216,vInf);
```



## The Verdict

```
t1Hr = StoH(tEsc);
t2Hr = StoH(tTsfr);
t3Hr = StoH(tCap);

t1D = StoD(tEsc);
t2D = StoD(tTsfr);
t3D = StoD(tCap);

tTotals = tEsc + tTsfr + tCap;
tTotalYr = StoYr(tTotals);

deltaV = dv1+dv4; % dv2 and 3 are left out because there is no
firing required in the hohmann transfer

sprintf('The escape phase requires %Gm/s and takes %G
hr',dvl,t1Hr) sprintf('The Hohmann transfer phase requires %Gm/s
```

```

and takes %G days',0,t2D)
sprintf('The capture phase requires %Gm/s and takes %G
hr',dv4,t3Hr) sprintf('The entire mission (escape to capture)
requires %Gm/s and takes %G years',deltaV,tTotalYr)
sprintf('More #V is required to utilize payload in a similar
fashion to Psyche Mission, but these results are quite
heartening')

ans =
'The escape phase requires 166.815m/s and takes 22.8189 hr'

ans =
'The Hohmann transfer phase requires 0m/s and takes 955.293 days'

ans =
'The capture phase requires 808.063m/s and takes 2.73438 hr'

ans =
'The entire mission (escape to capture) requires 974.878m/s and
takes 2.62016 years'

ans =
'More #V is required to utilize payload in a similar fashion to
Psyche Mission, but these results are quite heartening'

```

## Functions

```

% E = -mu^2/(2H^2) % for circles only (eccentricity = 0)
% with thanks to Marti Sarigul-Klijn for the formula

function Vr = Oberth(mu,r,Vinf)
Vr = ((escapeVelocity(mu,r))^2+Vinf^2)^0.5;
end

function Vesc = escapeVelocity(mu,r)
Vesc = (2*mu/r)^0.5;
end

function Vcirc = circularVelocity(mu,r)
Vcirc = (mu/r)^0.5;
end

```

```

function E = energyl(mu,a)
E = -mu/(2*a);
end

function E = energy2(V,mu,r)
E = V^2/2-mu/r;
end

function Einf = energyInfinity(Vinf)
% where Vinf is the velocity at r = infinity
Einf = Vinf^2/2;
end

function p = semilatus1(a,epsilon)
% semilatus rectum, distance above foci
p = a*(1-epsilon^2);
end

function p = semilatus2(H,mu)
% semilatus rectum, distance above foci
p = H^2/mu;
end

function e = eccentricity1(ra,rp)
e = (ra-rp)/(ra+rp);
end

function e = eccentricity2(E,H,mu)
e = (1+(2*E*H^2/mu^2))^.5;
end

function H = angularMomentum4(va,ra)
% works at both apogee and perogee
H = va*ra;
end

function a = majorAxisHalf1(ra,rp) % where 2a is the major
axis a = (ra+rp)/2;
end

function a = majorAxisHalf2(p,e) % where 2a is the major
axis a = p/(1-e^2);
end

function a = majorAxisHalf3(mu,E) % where 2a is the major
axis a = -mu/(2*E);
end

function rp = radiusPeriapsis(a,e) % smallest radius in
orbit rp = a*(1-e);
end

```

```

function V = velocity(E,mu,r) % general radius
V = (2*(E+mu/r))^0.5;
end

function x = parax(rho,theta)
x = rho.*cos(theta);
end

function y = paray(rho,theta)
y = rho.*sin(theta);
end

function [x,y] = para(rho,theta)
x = rho.*cos(theta);
y = rho.*sin(theta);
end

function [x,y] = paraHyperbola(a,p)
x = linspace(a, 2*a,1000);
b = bGeo(a,p);
c = (a^2+b^2)^0.5;
y = b*(x.^2./a^2-1).^0.5;
x = x+c;
end

function m = AUtoM(AU)
% from
https://ssd.jpl.nasa.gov/tools/sbdb\_lookup.html#/?sstr=16&view=OPDA
% convert astronomical units to meters
m = AU*149597870.70*1000;
end

function r = SOI(m2,m1,a)
% where m2 is the smaller mass, m1 is the larger mass, and a is
% the % semi-major axis of m2 revolving m1
r = a*(m2/m1)^0.4;
end

function b = bGeo(a,p)
b = (abs(a)*p)^0.5;
end

function t = TOF_ellipse(a,mu)
t = 2*pi*(a^3/mu)^0.5;
end

function nu = trueAnomoly(e,p,r)
nu = acos(1/e*(p/r-1));
end

```

```

function tof = TOF_hyp(mu,mu,e,a)
% to find the hyperbolic time of flight from periapsis to point
A % thus nu should be the true anomoly at point A

coshf = (e+cos(nu))/(1+e*cos(nu));
F = acosh(coshf);
M = e*sinh(F)-F;
tof = M*((-a)^3/mu)^0.5;

end

function hr = StoH(s)
hr = s/(60*60);
end

function hr = StoD(s)
hr = s/(60*60*24);
end

function hr = StoYr(s)
hr = s/(60*60*24*365);
end

function v = derivedV(mu,a,r)
% derived formula for v(mu,a,r) in order to minimize truncation
error v = (mu*(2*a-r)/(a*r))^0.5;
end

function b = impactParameter(vInf,mu,r)
vEsc = escapeVelocity(mu,r);
b = r*(1+vEsc^2/vInf^2)^0.5;
end

function [dv1,tEsc] =
escape(mu,muSun,rOrbitD,Vinf,r16,a16) % planet centric
calculations

Vcirc = circularVelocity(mu,rOrbitD); % velocity of spacecraft orbit
D Vob = Oberth(mu,rOrbitD,Vinf); % velocity needed to escape 16
psyche dv1 = abs(Vob-Vcirc);

% orbit characteristics

E = energyInfinity(Vinf);
H = angularMomentum4(Vob,rOrbitD);
e = eccentricity2(E,H,mu);
p = semilatus2(H,mu);
a = majorAxisHalf2(p,e);

% TOF
soi = SOI(mu,muSun,a16);
nu = trueAnomoly(e,p,soi);
tEsc = TOF_hyp(nu,mu,e,a);

```

```
% graph

theta = linspace(0,2*pi,500);
[dx,dy] = para(rOrbitD,theta); % orbit D x and y
psy_y = paray(r16,theta); % psyche y data
[ex,ey] = paraHyperbola(a,p); % escape x and y

figure
title(sprintf('16 Psyche Escape from Orbit D Vinf = %g m/s, \mu
= %g',Vinf, mu))
hold on
plot(dx,dy,'b','LineWidth',2) % orbit D
for i = 1:100:r16 % plot psyche as cyan
    psy_x = parax(i,theta);
    plot(psy_x,psy_y,'c')
end
plot(ex,ey, 'r','LineWidth',2) % escape
xlabel('m')
ylabel('m')
set(gca, 'color', [0,0,0])
axis equal
hold off

end

function [dv1,dv2,tTsfr,va16,va216,vp16,vp216,vaTsfr] =
transfer(a216,ra216,rp216,e216,a16,ra16,rp16,e16,rSun,muSun) % for
inner or outer hohman transfer orbit, from ellipse to ellipse %
sun centric calculations

E16 = energy1(muSun,a16);
E216 = energy1(muSun,a216);

check = E16 > E216;

switch check
case 1 % fire opposite direction of planet

    % outer asteroid
    va16 = derivedV(muSun,a16,ra16);
    vp16 = derivedV(muSun,a16,rp16);
    p16 = semilatus1(a16,e16);

    % inner asteroid
    va216 = derivedV(muSun,a216,ra216);
    vp216 = derivedV(muSun,a216,rp216);
    p216 = semilatus1(a216,e216);

    % Hohman transfer orbit
```

```

rpTsfr = rp16; % by nature of inner orbit geometry firing at
apogee
raTsfr = ra216; % by nature of inner orbit geometry firing at
apogee
% for some reason this only works with overlapping ellipses. This
% is the case we find ourselves in, but do not use this code 10

%
% blindly later. It appears swapping raTsfr and rpTsfr does the
% trick but since I can't tell when it will overlap, I can't tell
% whether it will work and when it won't

eTsfr = eccentricity1(raTsfr,rpTsfr);
aTsfr = majorAxisHalf1(raTsfr,rpTsfr);
pTsfr = semilatus1(aTsfr,eTsfr);
vaTsfr = derivedV(muSun,aTsfr,raTsfr);
vpTsfr = derivedV(muSun,aTsfr,rpTsfr);

tTsfr = TOF_ellipse(aTsfr,muSun)/2;
t16 = TOF_ellipse(a16,muSun)/2;

dv1 = abs(vp16-vpTsfr); % dv leaving psyche dv2 =
abs(vaTsfr-va216); % dv to enter kleopatra

theta = linspace(0,2*pi,500);

bTsfr = bGeo(aTsfr,pTsfr);
cTsfr = (aTsfr^2-bTsfr^2)^0.5;

xTsfr = (aTsfr)*cos(theta)-cTsfr; % since a > b, focus (sun) is
offset on the x axis
yTsfr = (bTsfr)*sin(theta);

b16 = bGeo(a16,p16);
c16 = (a16^2-b16^2)^0.5;

x16 = (a16)*cos(theta)-c16; % since a > b, focus (sun) is
offset on the x axis
y16 = (b16)*sin(theta);

b216 = bGeo(a216,p216);
c216 = (a216^2-b216^2)^0.5;

x216 = (a216)*cos(theta)-c216; % since a > b, focus (sun) is
offset on the x axis
y216 = (b216)*sin(theta);

```

```
% graph

theta = linspace(0,2*pi,500);
sun_y = paray(rSun,theta); % sun y data
sun_x = parax(rSun,theta);

figure
title(sprintf('Orbital Transfer From 16 Psyche to 216
Kleopatra'))
hold on
plot(x16,y16,'b','Linewidth',2) % 16 Psyche orbit blue
plot(x216,y216,'g','Linewidth',2) % 216 Kleopatra orbit green
plot(xTsfr,yTsfr,'r','Linewidth',2) % transfer orbit red
plot(sun_x,sun_y,'y','Linewidth',2)

% temp = linspace(1,rSun,length(1:1000000:rSun)); % for i =
1:length(1:1000000:rSun) % plot sun as yellow %
% sun_x = parax(temp(i),theta);
% plot(sun_x,sun_y,'y')
%
% end

xlabel('m')
ylabel('m')
set(gca, 'color', [0,0,0])
axis equal
lgd = legend('16 Psyche','216 Kleopatra','Transfer
Orbit','Sun');
%c = lgd.TextColor;
lgd.TextColor = [1,1,1];
hold off

case 0 % fire same direction as asteroid

% inner asteroid
va16 = derivedV(muSun,a16,ra16);
vp16 = derivedV(muSun,a16,rp16);
p16 = semilatus1(a16,e16);

% outer asteroid
va216 = derivedV(muSun,a216,ra216);
vp216 = derivedV(muSun,a216,rp216);
p216 = semilatus1(a216,e216);

% Hohman transfer orbit
rpTsfr = rp16; % by nature of outer orbit geometry firing at
apogee
raTsfr = ra216; % by nature of outer orbit geometry firing at
apogee

eTsfr = eccentricity1(raTsfr,rpTsfr);
```

```

aTsfr = majorAxisHalf1(raTsfr,rpTsfr);
pTsfr = semilatus1(aTsfr,eTsfr);
vaTsfr = derivedV(muSun,aTsfr,raTsfr);
vpTsfr = derivedV(muSun,aTsfr,rpTsfr);

tTsfr = TOF_ellipse(aTsfr,muSun)/2;
t16 = TOF_ellipse(a16,muSun)/2;
dv1 = abs(vp16-vpTsfr); % dv leaving psyche
dv2 = abs(vaTsfr-va216); % dv to enter kleopatra

theta = linspace(0,2*pi,500);

bTsfr = bGeo(aTsfr,pTsfr);
cTsfr = (aTsfr^2-bTsfr^2)^0.5;

xTsfr = (aTsfr)*cos(theta)-cTsfr; % since a > b, focus (sun) is
offset on the x axis
yTsfr = (bTsfr)*sin(theta);

b16 = bGeo(a16,p16);
c16 = (a16^2-b16^2)^0.5;

x16 = (a16)*cos(theta)-c16; % since a > b, focus (sun) is
offset on the x axis
y16 = (b16)*sin(theta);

b216 = bGeo(a216,p216);
c216 = (a216^2-b216^2)^0.5;

x216 = (a216)*cos(theta)-c216; % since a > b, focus (sun) is
offset on the x axis
y216 = (b216)*sin(theta);

% graph

theta = linspace(0,2*pi,500);
sun_y = paray(rSun,theta); % sun y data

figure
title(sprintf('Orbital Transfer From 16 Psyche to Outer
Orbit'))
hold on
plot(x16,y16,'b','Linewidth',2) % 16 Psyche orbit blue
plot(x216,y216,'g','Linewidth',2) % 216 Kleopatra orbit green
plot(xTsfr,yTsfr,'r','Linewidth',2) % transfer orbit red

temp = linspace(1,rSun,length(1:1000000:rSun)); for i =
1:length(1:1000000:rSun) % plot sun as yellow

sun_x = parax(temp(i),theta);

```

```

plot(sun_x,sun_y,'y')

end

xlabel('m')
ylabel('m')
set(gca, 'color', [0,0,0])
axis equal
legend off
hold off

end

end

function [dv4,tCap,rp] =
capture(mu216,muSun,a216,r216,vInf) soi216 =
SOI(mu216,muSun,a216);
b216 = impactParameter(vInf,mu216,r216);

% pick d! i chose half the distance between b and soi, but can
be weighted
% accordingly
d = b216 + 0.50*(soi216-b216);

% find dv to enter circular orbit, graph resulting trajectories

% incoming flyby
E = energy2(vInf,mu216,soi216);
H = angularMomentum4(vInf,d);
p = semilatus2(H,mu216);
e = eccentricity2(E,H,mu216);
a = majorAxisHalf3(mu216,E);
rp = radiusPeriapsis(a,e);
vp = velocity(E,mu216,rp);

% colinear firing
vcs = circularVelocity(mu216, rp);

dv4 = abs(vp-vcs);

% TOF

nu = trueAnomoly(e,p,soi216);
tCap = TOF_hyp(nu,mu216,e,a);

% graph

theta = linspace(0,2*pi,500);
[dx,dy] = para(rp,theta); % orbit D x and y
psy_y = paray(r216,theta); % psyche y data
[ex,ey] = paraHyperbola(a,p); % escape x and y

```

```
figure
title(sprintf('216 Kleopatra Capture with Vinf = %g, circular park
at %gm',vInf,rp))
hold on
plot(dx,dy,'b','LineWidth',2) % orbit D
for i = 1:100:r216 % plot kleopatra as cyan
    psy_x = parax(i,theta);
    plot(psy_x,psy_y,'c')
end

plot(ex,ey, 'r','LineWidth',2) %
escape xlabel('m')
ylabel('m')
set(gca, 'color', [0,0,0])
axis equal
hold off

end
```

*Published with MATLAB® R2020b*